Neutrino Mixing

INTRODUCTION TO NEUTRINO MIXING LISTINGS

Based on the discussion in the previous review "Understanding Two-Flavor Oscillation Parameters and Limits" by Don Groom, most results in the neutrino mixing listings are presented as Δm^2 limits (or ranges) for $\sin^2 2\theta = 1$, and $\sin^2 2\theta$ limits (or ranges) for large Δm^2. Together, they summarize most of the information contained in the usual Δm^2 vs $\sin^2 2\theta$ plots in the experiments' papers. The neutrino mixing listings are divided into four sub-sections:

(A) Accelerator neutrino experiments: shows Δm^2 and $\sin^2 2\theta$ limits for, successively, $\nu_e \to \nu_\tau$ and $\overline{\nu}_e \to \overline{\nu}_\tau$ appearance, $\nu_e \not\to \nu_e$ disappearance, $\nu_\mu \to \nu_e$, $\overline{\nu}_\mu \to \overline{\nu}_e$, $\nu_\mu \to \nu_\tau$ and $\overline{\nu}_\mu \to \overline{\nu}_\tau$ appearance, and $\nu_\mu \not\to \nu_\mu$ and $\overline{\nu}_\mu \not\to \overline{\nu}_\mu$ disappearance. They are all limits, except for the positive $\nu_\mu \not\to \nu_\mu$ signal from the K2K collaboration reported in AHN 03.

(B) Reactor $\overline{\nu}_e$ disappearance experiments: has Δm^2 and $\sin^2 2\theta$ limits for $\overline{\nu}_e \not\to \overline{\nu}_e$ disappearance, together with the ratios of measured to expected rates of events. It also contains the positive signal from the KamLAND collaboration (EGUCHI 03).

(C) Atmospheric neutrino observations: lists the ratio of measured to expect ν_μ rate, the double ratio of measured ν_μ/ν_e rates over expected, and the up/down ratio of measured over expected for both ν_μ and ν_e. It also gives Δm^2 and $\sin^2 2\theta$ limits for $\nu_e \leftrightarrow \nu_\mu$ and $\overline{\nu}_e \leftrightarrow \overline{\nu}_\mu$, as well as the Kamiokande, SuperKamiokande and MACRO measurements of both $\sin^2 2\theta$

and Δm^2 for $\nu_\mu \leftrightarrow \nu_\tau$ oscillations, together with limits on ν_μ oscillations to a sterile neutrino.

(D) Solar ν experiments: is organized differently, showing first the results from radiochemical experiments and moving then to results of ^{8}B fluxes from elastic scattering, charged current and neutral current. From these, the solar fluxes for all three neutrino flavors combined and for only ν_μ and ν_τ are derived and listed. The day/night asymmetry for ^{8}B is also listed. Finally, the Kamiokande limit on the "hep" ν_e flux from the sun as measured in elastic scattering is given.

(A) Accelerator neutrino experiments

$\nu_e \rightarrow \nu_\tau$

$\Delta(m^2)$ for $\sin^2(2\theta) = 1$

VALUE (eV^2)	*CL%*	*DOCUMENT ID*		*TECN*	*COMMENT*
< 0.77	90	[1] ARMBRUSTER	98	KARM	
• • • We do not use the following data for averages, fits, limits, etc. • • •					
< 5.9	90	[2] ASTIER	01B	NOMD	CERN SPS
< 7.5	90	[3] ESKUT	01	CHRS	CERN SPS
<17	90	NAPLES	99	CCFR	FNAL
<44	90	TALEBZADEH	87	HLBC	BEBC
< 9	90	USHIDA	86C	EMUL	FNAL

[1] ARMBRUSTER 98 use KARMEN detector with ν_e from muon decay at rest and observe $^{12}C(\nu_e,e^-)^{12}N_{gs}$. This is a disappearance experiment which is almost insensitive to $\nu_e \rightarrow \nu_\mu$ oscillation. Results are presented as limits to $\nu_e \rightarrow \nu_\tau$ oscillation, although the (non)oscillation could be to a non-visible flavor. A three-flavor analysis is also presented.

[2] ASTIER 01B searches for the appearance of ν_τ with the NOMAD detector at CERN's SPS. The limit is based on an oscillation probability $< 0.74 \times 10^{-2}$, whereas the quoted sensitivity was 1.1×10^{-2}. The limit was obtained following the statistical prescriptions of FELDMAN 98. See also the footnote to ESKUT 01.

[3] ESKUT 01 searches for the appearance of the ν_τ with the CHORUS detector at CERN's SPS. The limit is obtained following the statistical prescriptions in JUNK 99. The limit would have been 6 eV^2 if the prescriptions in FELDMAN 98 had been followed, as they were in ASTIER 01B.

$\sin^2(2\theta)$ for "Large" $\Delta(m^2)$

VALUE	*CL%*	*DOCUMENT ID*		*TECN*	*COMMENT*
<0.015	90	[4] ASTIER	01B	NOMD	CERN SPS

• • • We do not use the following data for averages, fits, limits, etc. • • •

<0.052	90	[5] ESKUT	01	CHRS	CERN SPS
<0.21	90	NAPLES	99	CCFR	FNAL
<0.338	90	[6] ARMBRUSTER	98	KARM	
<0.36	90	TALEBZADEH	87	HLBC	BEBC
<0.25	90	[7] USHIDA	86C	EMUL	FNAL

[4] ASTIER 01B limit is based on an oscillation probability $< 0.74 \times 10^{-2}$, whereas the quoted sensitivity was 1.1×10^{-2}. The limit was obtained following the statistical prescriptions of FELDMAN 98. See also the footnote to ESKUT 01.

[5] ESKUT 01 limit obtained following the statistical prescriptions in JUNK 99. The limit would have been 0.03 if the prescriptions in FELDMAN 98 had been followed, as they were in ASTIER 01B.

[6] See footnote in preceding table (ARMBRUSTER 98) for further details, and see the paper for a plot showing allowed regions. A three-flavor analysis is also presented here.

[7] USHIDA 86C published result is $\sin^2 2\theta < 0.12$. The quoted result is corrected for a numerical mistake incurred in calculating the expected number of ν_e CC events, normalized to the total number of neutrino interactions (3886) rather than to the total number of ν_μ CC events (1870).

$\overline{\nu}_e \to \overline{\nu}_\tau$

$\sin^2(2\theta)$ for "Large" $\Delta(m^2)$

VALUE	CL%	DOCUMENT ID		TECN	COMMENT
<0.7	90	[8] FRITZE	80	HYBR	BEBC CERN SPS

[8] Authors give $P(\nu_e \to \nu_\tau) < 0.35$, equivalent to above limit.

$\nu_e \not\to \nu_e$

$\Delta(m^2)$ for $\sin^2(2\theta) = 1$

VALUE (eV^2)	CL%	DOCUMENT ID		TECN	COMMENT
< 0.18	90	[9] HAMPEL	98	GALX	[51]Cr source

• • • We do not use the following data for averages, fits, limits, etc. • • •

<40	90	[10] BORISOV	96	CNTR	IHEP-JINR detector
<14.9	90	BRUCKER	86	HLBC	15-ft FNAL
< 8	90	BAKER	81	HLBC	15-ft FNAL
<56	90	DEDEN	81	HLBC	BEBC CERN SPS
<10	90	ERRIQUEZ	81	HLBC	BEBC CERN SPS
<2.3 OR >8	90	NEMETHY	81B	CNTR	LAMPF

[9] HAMPEL 98 analyzed the GALLEX calibration results with [51]Cr neutrino sources and updates the BAHCALL 95 analysis result. They also gave 95% and 99% CL limits of < 0.2 and < 0.22, respectively.

[10] BORISOV 96 exclusion curve extrapolated to obtain this value; however, it does not have the right curvature in this region.

$\sin^2(2\theta)$ for "Large" $\Delta(m^2)$

VALUE	CL%	DOCUMENT ID		TECN	COMMENT
<7 $\times 10^{-2}$	90	[11] ERRIQUEZ	81	HLBC	BEBC CERN SPS

• • • We do not use the following data for averages, fits, limits, etc. • • •

<0.4	90	[12] HAMPEL	98	GALX	^{51}Cr source
<0.115	90	[13] BORISOV	96	CNTR	$\Delta(m^2) = 175$ eV^2
<0.54	90	BRUCKER	86	HLBC	15-ft FNAL
<0.6	90	BAKER	81	HLBC	15-ft FNAL
<0.3	90	[11] DEDEN	81	HLBC	BEBC CERN SPS

[11] Obtained from a Gaussian centered in the unphysical region.

[12] HAMPEL 98 analyzed the GALLEX calibration results with ^{51}Cr neutrino sources and updates the BAHCALL 95 analysis result. They also gave 95% and 99% CL limits of < 0.45 and < 0.56, respectively.

[13] BORISOV 96 sets less stringent limits at large $\Delta(m^2)$, but exclusion curve does not have clear asymptotic behavior.

$\nu_e \rightarrow (\overline{\nu}_e)_L$

This is a limit on lepton family-number violation and total lepton-number violation. $(\overline{\nu}_e)_L$ denotes a hypothetical left-handed $\overline{\nu}_e$. The bound is quoted in terms of Δ (m^2), $\sin(2\theta)$, and α, where α denotes the fractional admixture of $(V+A)$ charged current.

$\alpha\Delta(m^2)$ for $\sin^2(2\theta) = 1$

VALUE (eV^2)	*CL%*	*DOCUMENT ID*		*TECN*	*COMMENT*
<0.14	90	[14] FREEDMAN	93	CNTR	LAMPF

• • • We do not use the following data for averages, fits, limits, etc. • • •

<7	90	[15] COOPER	82	HLBC	BEBC CERN SPS

[14] FREEDMAN 93 is a search at LAMPF for $\overline{\nu}_e$ generated from any of the three neutrino types ν_μ, $\overline{\nu}_\mu$, and ν_e which come from the beam stop. The $\overline{\nu}_e$'s would be detected by the reaction $\overline{\nu}_e p \rightarrow e^+ n$.

[15] COOPER 82 states that existing bounds on V+A currents require α to be small.

$\alpha^2\sin^2(2\theta)$ for "Large" $\Delta(m^2)$

VALUE	*CL%*	*DOCUMENT ID*		*TECN*	*COMMENT*
<0.032	90	[16] FREEDMAN	93	CNTR	LAMPF

• • • We do not use the following data for averages, fits, limits, etc. • • •

<0.05	90	[17] COOPER	82	HLBC	BEBC CERN SPS

[16] FREEDMAN 93 is a search at LAMPF for $\overline{\nu}_e$ generated from any of the three neutrino types ν_μ, $\overline{\nu}_\mu$, and ν_e which come from the beam stop. The $\overline{\nu}_e$'s would be detected by the reaction $\overline{\nu}_e p \rightarrow e^+ n$.

[17] COOPER 82 states that existing bounds on V+A currents require α to be small.

$\nu_\mu \rightarrow \nu_e$

$\Delta(m^2)$ for $\sin^2(2\theta) = 1$

VALUE (eV^2)	*CL%*	*DOCUMENT ID*		*TECN*	*COMMENT*
<0.09	90	ANGELINI	86	HLBC	BEBC CERN PS

• • • We do not use the following data for averages, fits, limits, etc. • • •

<0.4	90		ASTIER	03	NOMD	CERN SPS
<2.4	90		AVVAKUNOV	02	NTEV	NUTEV FNAL
		[18]	AGUILAR	01	LSND	$\nu\mu \rightarrow \nu_e$ osc.prob.
0.03 to 0.3	95	[19]	ATHANASSO...	98	LSND	$\nu_\mu \rightarrow \nu_e$
<2.3	90	[20]	LOVERRE	96		CHARM/CDHS
<0.9	90		VILAIN	94C	CHM2	CERN SPS
<0.1	90		BLUMENFELD	89	CNTR	
<1.3	90		AMMOSOV	88	HLBC	SKAT at Serpukhov
<0.19	90		BERGSMA	88	CHRM	
		[21]	LOVERRE	88	RVUE	
<2.4	90		AHRENS	87	CNTR	BNL AGS
<1.8	90		BOFILL	87	CNTR	FNAL
<2.2	90	[22]	BRUCKER	86	HLBC	15-ft FNAL
<0.43	90		AHRENS	85	CNTR	BNL AGS E734
<0.20	90		BERGSMA	84	CHRM	
<1.7	90		ARMENISE	81	HLBC	GGM CERN PS
<0.6	90		BAKER	81	HLBC	15-ft FNAL
<1.7	90		ERRIQUEZ	81	HLBC	BEBC CERN PS
<1.2	95		BLIETSCHAU	78	HLBC	GGM CERN PS
<1.2	95		BELLOTTI	76	HLBC	GGM CERN PS

[18] AGUILAR 01 is the final analysis of the LSND full data set. Search is made for the $\nu_\mu \rightarrow \nu_e$ oscillations using ν_μ from π^+ decay in flight by observing beam-on electron events from $\nu_e C \rightarrow e^- X$. Present analysis results in $8.1 \pm 12.2 \pm 1.7$ excess events in the $60 < E_e < 200$ MeV energy range, corresponding to oscillation probability of $0.10 \pm 0.16 \pm 0.04\%$. This is consistent, though less significant, with the previous result of ATHANASSOPOULOS 98, which it supersedes. The present analysis uses selection criteria developed for the decay at rest region, and is less effective in removing the background above 60 MeV than ATHANASSOPOULOS 98.

[19] ATHANASSOPOULOS 98 is a search for the $\nu_\mu \rightarrow \nu_e$ oscillations using ν_μ from π^+ decay in flight. The 40 observed beam-on electron events are consistent with $\nu_e C \rightarrow e^- X$; the expected background is 21.9 ± 2.1. Authors interpret this excess as evidence for an oscillation signal corresponding to oscillations with probability $(0.26 \pm 0.10 \pm 0.05)\%$. Although the significance is only $2.3\,\sigma$, this measurement is an important and consistent cross check of ATHANASSOPOULOS 96 who reported evidence for $\overline{\nu}_\mu \rightarrow \overline{\nu}_e$ oscillations from μ^+ decay at rest. See also ATHANASSOPOULOS 98B.

[20] LOVERRE 96 uses the charged-current to neutral-current ratio from the combined CHARM (ALLABY 86) and CDHS (ABRAMOWICZ 86) data from 1986.

[21] LOVERRE 88 reports a less stringent, indirect limit based on theoretical analysis of neutral to charged current ratios.

[22] 15ft bubble chamber at FNAL.

$\sin^2(2\theta)$ for "Large" $\Delta(m^2)$

VALUE (units 10^{-3})	CL%	DOCUMENT ID		TECN	COMMENT
< 1.4	90	ASTIER	03	NOMD	CERN SPS

• • • We do not use the following data for averages, fits, limits, etc. • • •

$<$ 1.6		90		AVVAKUNOV	02	NTEV NUTEV FNAL
			[23]	AGUILAR	01	LSND $\nu\mu \rightarrow \nu_e$ osc.prob.
0.5 to 30		95	[24]	ATHANASSO...	98	LSND $\nu_\mu \rightarrow \nu_e$
$<$ 3.0		90	[25]	LOVERRE	96	CHARM/CDHS
$<$ 9.4		90		VILAIN	94C	CHM2 CERN SPS
$<$ 5.6		90	[26]	VILAIN	94C	CHM2 CERN SPS
$<$ 16		90		BLUMENFELD	89	CNTR
$<$ 2.5		90		AMMOSOV	88	HLBC SKAT at Serpukhov
$<$ 8		90		BERGSMA	88	CHRM $\Delta(m^2) \geq$ 30 eV^2
			[27]	LOVERRE	88	RVUE
$<$ 10		90		AHRENS	87	CNTR BNL AGS
$<$ 15		90		BOFILL	87	CNTR FNAL
$<$ 20		90	[28]	ANGELINI	86	HLBC BEBC CERN PS
20	to 40		[29]	BERNARDI	86B	CNTR $\Delta(m^2)$=5–10
$<$ 11		90	[30]	BRUCKER	86	HLBC 15-ft FNAL
$<$ 3.4		90		AHRENS	85	CNTR BNL AGS E734
$<$240		90		BERGSMA	84	CHRM
$<$ 10		90		ARMENISE	81	HLBC GGM CERN PS
$<$ 6		90		BAKER	81	HLBC 15-ft FNAL
$<$ 10		90		ERRIQUEZ	81	HLBC BEBC CERN PS
$<$ 4		95		BLIETSCHAU	78	HLBC GGM CERN PS
$<$ 10		95		BELLOTTI	76	HLBC GGM CERN PS

[23] AGUILAR 01 is the final analysis of the LSND full data set of the search for the $\nu_\mu \rightarrow \nu_e$ oscillations. See footnote in preceding table for further details.

[24] ATHANASSOPOULOS 98 report $(0.26 \pm 0.10 \pm 0.05)$% for the oscillation probability; the value of $\sin^2 2\theta$ for large Δm^2 is deduced from this probability. See footnote in preceding table for further details, and see the paper for a plot showing allowed regions. If effect is due to oscillation, it is most likely to be intermediate $\sin^2 2\theta$ and Δm^2. See also ATHANASSOPOULOS 98B.

[25] LOVERRE 96 uses the charged-current to neutral-current ratio from the combined CHARM (ALLABY 86) and CDHS (ABRAMOWICZ 86) data from 1986.

[26] VILAIN 94C limit derived by combining the ν_μ and $\overline{\nu}_\mu$ data assuming *CP* conservation.

[27] LOVERRE 88 reports a less stringent, indirect limit based on theoretical analysis of neutral to charged current ratios.

[28] ANGELINI 86 limit reaches 13×10^{-3} at $\Delta(m^2) \approx 2$ eV^2.

[29] BERNARDI 86B is a typical fit to the data, assuming mixing between two species. As the authors state, this result is in conflict with earlier upper bounds on this type of neutrino oscillations.

[30] 15ft bubble chamber at FNAL.

$\overline{\nu}_\mu \rightarrow \overline{\nu}_e$

$\Delta(m^2)$ for $\sin^2(2\theta) = 1$

VALUE (eV^2)	*CL%*	*DOCUMENT ID*		*TECN*	*COMMENT*
<0.055	90	[31]	ARMBRUSTER02	KAR2	Liquid Sci. calor.

• • • We do not use the following data for averages, fits, limits, etc. • • •

<2.6	90	AVVAKUNOV	02	NTEV	NUTEV FNAL
0.03–0.05		[32] AGUILAR	01	LSND	LAMPF
0.05–0.08	90	[33] ATHANASSO...	96	LSND	LAMPF
0.048–0.090	80	[34] ATHANASSO...	95		
<0.07	90	[35] HILL	95		
<0.9	90	VILAIN	94C	CHM2	CERN SPS
<0.14	90	[36] FREEDMAN	93	CNTR	LAMPF
<3.1	90	BOFILL	87	CNTR	FNAL
<2.4	90	TAYLOR	83	HLBC	15-ft FNAL
<0.91	90	[37] NEMETHY	81B	CNTR	LAMPF
<1	95	BLIETSCHAU	78	HLBC	GGM CERN PS

[31] ARMBRUSTER 02 is the final analysis of the KARMEN 2 data for 17.7 m distance from the ISIS stopped pion and muon neutrino source. It is a search for $\overline{\nu}_e$, detected by the inverse β-decay reaction on protons and ^{12}C. 15 candidate events are observed, and 15.8 $\pm$ 0.5 background events are expected, hence no oscillation signal is detected. The results exclude large regions of the parameter area favored by the LSND experiment.

[32] AGUILAR 01 is the final analysis of the LSND full data set. It is a search for $\overline{\nu}_e$ 30 m from LAMPF beam stop. Neutrinos originate mainly for π^+ decay at rest. $\overline{\nu}_e$ are detected through $\overline{\nu}_e p \rightarrow e^+ n$ ($20 < E_{e^+} < 60$ MeV) in delayed coincidence with $np \rightarrow d\gamma$. AUthors observe 87.9 $\pm$ 22.4 $\pm$ 6.0 total excess events. The observation is attributed to $\overline{\nu}_\mu \rightarrow \overline{\nu}_e$ oscillations with the oscillation probability of 0.264 $\pm$ 0.067 $\pm$ 0.045%, consistent with the previously published result. Taking into account all constraints, the most favored allowed region of oscillation parameters is a band of $\Delta(m^2)$ from 0.2–2.0 eV^2. Supersedes ATHANASSOPOULOS 95, ATHANASSOPOULOS 96, and ATHANASSOPOULOS 98.

[33] ATHANASSOPOULOS 96 is a search for $\overline{\nu}_e$ 30 m from LAMPF beam stop. Neutrinos originate mainly from π^+ decay at rest. $\overline{\nu}_e$ could come from either $\overline{\nu}_\mu \rightarrow \overline{\nu}_e$ or $\nu_e \rightarrow \overline{\nu}_e$; our entry assumes the first interpretation. They are detected through $\overline{\nu}_e p \rightarrow e^+ n$ (20 MeV $< E_{e^+} <$60 MeV) in delayed coincidence with $np \rightarrow d\gamma$. Authors observe 51 $\pm$ 20 $\pm$ 8 total excess events over an estimated background 12.5 $\pm$ 2.9. ATHANASSOPOULOS 96B is a shorter version of this paper.

[34] ATHANASSOPOULOS 95 error corresponds to the 1.6σ band in the plot. The expected background is 2.7 $\pm$ 0.4 events. Corresponds to an oscillation probability of $(0.34^{+0.20}_{-0.18} \pm 0.07)$%. For a different interpretation, see HILL 95. Replaced by ATHANASSOPOULOS 96.

[35] HILL 95 is a report by one member of the LSND Collaboration, reporting a different conclusion from the analysis of the data of this experiment (see ATHANASSOPOULOS 95). Contrary to the rest of the LSND Collaboration, Hill finds no evidence for the neutrino oscillation $\overline{\nu}_\mu \rightarrow \overline{\nu}_e$ and obtains only upper limits.

[36] FREEDMAN 93 is a search at LAMPF for $\overline{\nu}_e$ generated from any of the three neutrino types ν_μ, $\overline{\nu}_\mu$, and ν_e which come from the beam stop. The $\overline{\nu}_e$'s would be detected by the reaction $\overline{\nu}_e p \rightarrow e^+ n$. FREEDMAN 93 replaces DURKIN 88.

[37] In reaction $\overline{\nu}_e p \rightarrow e^+ n$.

$\sin^2(2\theta)$ for "Large" $\Delta(m^2)$

VALUE	CL%	DOCUMENT ID		TECN	COMMENT
<0.0011	90	AVVAKUNOV	02	NTEV	NUTEV FNAL

• • • We do not use the following data for averages, fits, limits, etc. • • •

<0.0017	90	[38]	ARMBRUSTER	02	KAR2	Liquid Sci. calor.
0.0053 ± 0.0013 ± 0.009		[39]	AGUILAR	01	LSND	LAMPF
0.0062 ± 0.0024 ± 0.0010		[40]	ATHANASSO...	96	LSND	LAMPF
0.003–0.012	80	[41]	ATHANASSO...	95		
<0.006	90	[42]	HILL	95		
<4.8	90		VILAIN	94C	CHM2	CERN SPS
<5.6	90	[43]	VILAIN	94C	CHM2	CERN SPS
<0.024	90	[44]	FREEDMAN	93	CNTR	LAMPF
<0.04	90		BOFILL	87	CNTR	FNAL
<0.013	90		TAYLOR	83	HLBC	15-ft FNAL
<0.2	90	[45]	NEMETHY	81B	CNTR	LAMPF
<0.004	95		BLIETSCHAU	78	HLBC	GGM CERN PS

[38] ARMBRUSTER 02 is the final analysis of the KARMEN 2 data. See footnote in the preceding table for further details, and the paper for the exclusion plot.

[39] AGUILAR 01 is the final analysis of the LSND full data set. The deduced oscillation probability is $0.264 \pm 0.067 \pm 0.045\%$; the value of $\sin^2 2\theta$ for large $\Delta(m^2)$ is twice this probability (although these values are excluded by other constraints). See footnote in preceding table for further details, and the paper for a plot showing allowed regions. Supersedes ATHANASSOPOULOS 95, ATHANASSOPOULOS 96, and ATHANASSOPOULOS 98.

[40] ATHANASSOPOULOS 96 reports $(0.31 \pm 0.12 \pm 0.05)\%$ for the oscillation probability; the value of $\sin^2 2\theta$ for large $\Delta(m^2)$ should be twice this probability. See footnote in preceding table for further details, and see the paper for a plot showing allowed regions.

[41] ATHANASSOPOULOS 95 error corresponds to the 1.6σ band in the plot. The expected background is 2.7 ± 0.4 events. Corresponds to an oscillation probability of $(0.34^{+0.20}_{-0.18} \pm 0.07)\%$. For a different interpretation, see HILL 95. Replaced by ATHANASSOPOULOS 96.

[42] HILL 95 is a report by one member of the LSND Collaboration, reporting a different conclusion from the analysis of the data of this experiment (see ATHANASSOPOULOS 95). Contrary to the rest of the LSND Collaboration, Hill finds no evidence for the neutrino oscillation $\overline{\nu}_\mu \rightarrow \overline{\nu}_e$ and obtains only upper limits.

[43] VILAIN 94C limit derived by combining the ν_μ and $\overline{\nu}_\mu$ data assuming *CP* conservation.

[44] FREEDMAN 93 is a search at LAMPF for $\overline{\nu}_e$ generated from any of the three neutrino types ν_μ, $\overline{\nu}_\mu$, and ν_e which come from the beam stop. The $\overline{\nu}_e$'s would be detected by the reaction $\overline{\nu}_e p \rightarrow e^+ n$. FREEDMAN 93 replaces DURKIN 88.

[45] In reaction $\overline{\nu}_e p \rightarrow e^+ n$.

$\nu_\mu(\overline{\nu}_\mu) \rightarrow \nu_e(\overline{\nu}_e)$

$\Delta(m^2)$ for $\sin^2(2\theta) = 1$

VALUE (eV^2)	*CL%*	*DOCUMENT ID*		*TECN*	*COMMENT*
<0.075	90	BORODOV...	92	CNTR	BNL E776

• • • We do not use the following data for averages, fits, limits, etc. • • •

<1.6	90	[46]	ROMOSAN	97	CCFR	FNAL

[46] ROMOSAN 97 uses wideband beam with a 0.5 km decay region.

$\sin^2(2\theta)$ for "Large" $\Delta(m^2)$

VALUE (units 10^{-3})	CL%	DOCUMENT ID		TECN	COMMENT
<1.8	90	[47] ROMOSAN	97	CCFR	FNAL
• • • We do not use the following data for averages, fits, limits, etc. • • •					
<3.8	90	[48] MCFARLAND	95	CCFR	FNAL
<3	90	BORODOV...	92	CNTR	BNL E776

[47] ROMOSAN 97 uses wideband beam with a 0.5 km decay region.

[48] MCFARLAND 95 state that "This result is the most stringent to date for $250 < \Delta(m^2) < 450$ eV^2 and also excludes at 90%CL much of the high $\Delta(m^2)$ region favored by the recent LSND observation." See ATHANASSOPOULOS 95 and ATHANASSOPOULOS 96.

$\nu_\mu \rightarrow \nu_\tau$

$\Delta(m^2)$ for $\sin^2(2\theta) = 1$

VALUE (eV^2)	CL%	DOCUMENT ID		TECN	COMMENT
< 0.6	90	[49] ESKUT	01	CHRS	CERN SPS
• • • We do not use the following data for averages, fits, limits, etc. • • •					
< 0.7	90	[50] ASTIER	01B	NOMD	CERN SPS
< 1.4	90	[51] ALTEGOER	98B	NOMD	CERN SPS
< 1.5	90	[52] ESKUT	98	CHRS	CERN SPS
< 1.1	90	[53] ESKUT	98B	CHRS	CERN SPS
< 3.3	90	[54] LOVERRE	96		CHARM/CDHS
< 1.4	90	MCFARLAND	95	CCFR	FNAL
< 4.5	90	BATUSOV	90B	EMUL	FNAL
<10.2	90	BOFILL	87	CNTR	FNAL
< 6.3	90	BRUCKER	86	HLBC	15-ft FNAL
< 0.9	90	USHIDA	86C	EMUL	FNAL
< 4.6	90	ARMENISE	81	HLBC	GGM CERN SPS
< 3	90	BAKER	81	HLBC	15-ft FNAL
< 6	90	ERRIQUEZ	81	HLBC	BEBC CERN SPS
< 3	90	USHIDA	81	EMUL	FNAL

[49] ESKUT 01 limit obtained following the statistical prescriptions in JUNK 99. The limit would have been 0.5 eV^2 if the prescriptions in FELDMAN 98 had been followed, as they were in ASTIER 01B.

[50] ASTIER 01B limit is based on an oscillation probability $< 1.63 \times 10^{-4}$, whereas the quoted sensitivity was 2.5×10^{-4}. The limit was obtained following the statistical prescriptions of FELDMAN 98. See also the footnote to ESKUT 01.

[51] ALTEGOER 98B is the NOMAD 1995 data sample result, searching for events with $\tau^- \rightarrow e^- \nu_\tau \overline{\nu}_e$, hadron$^-$ ν_τ, or $\pi^- \pi^+ \pi^-$ decay modes using classical CL approach of FELDMAN 98.

[52] ESKUT 98 search for events with one μ^- with indication of a kink from τ^- decay in the nuclear emulsion. No candidates were found in a 31,423 event subsample.

[53] ESKUT 98B search for $\tau^- \rightarrow \mu^- \nu_\tau \overline{\nu}_\mu$ or $h^- \nu_\tau \overline{\nu}_\mu$, where h^- is a negatively charged hadron. The μ^- sample is somewhat larger than in ESKUT 98, which this result supersedes. Bayesian limit.

[54] LOVERRE 96 uses the charged-current to neutral-current ratio from the combined CHARM (ALLABY 86) and CDHS (ABRAMOWICZ 86) data from 1986.

$\sin^2(2\theta)$ for "Large" $\Delta(m^2)$

VALUE	CL%	DOCUMENT ID		TECN	COMMENT
<0.00033	90	[55] ASTIER	01B	NOMD	CERN SPS
• • • We do not use the following data for averages, fits, limits, etc. • • •					
<0.00068	90	[56] ESKUT	01	CHRS	CERN SPS
<0.0042	90	[57] ALTEGOER	98B	NOMD	CERN SPS
<0.0035	90	[58] ESKUT	98	CHRS	CERN SPS
<0.0018	90	[59] ESKUT	98B	CHRS	CERN SPS
<0.006	90	[60] LOVERRE	96		CHARM/CDHS
<0.0081	90	MCFARLAND	95	CCFR	FNAL
<0.06	90	BATUSOV	90B	EMUL	FNAL
<0.34	90	BOFILL	87	CNTR	FNAL
<0.088	90	BRUCKER	86	HLBC	15-ft FNAL
<0.004	90	USHIDA	86C	EMUL	FNAL
<0.11	90	BALLAGH	84	HLBC	15-ft FNAL
<0.017	90	ARMENISE	81	HLBC	GGM CERN SPS
<0.06	90	BAKER	81	HLBC	15-ft FNAL
<0.05	90	ERRIQUEZ	81	HLBC	BEBC CERN SPS
<0.013	90	USHIDA	81	EMUL	FNAL

[55] ASTIER 01B limit is based on an oscillation probability $< 1.63 \times 10^{-4}$, whereas the quoted sensitivity was 2.5×10^{-4}. The limit was obtained following the statistical prescriptions of FELDMAN 98. See also the footnote to ESKUT 01.

[56] ESKUT 01 limit obtained following the statistical prescriptions in JUNK 99. The limit would have been 0.00040 if the prescriptions in FELDMAN 98 had been followed, as they were in ASTIER 01B.

[57] ALTEGOER 98B is the NOMAD 1995 data sample result, searching for events with $\tau^- \to e^- \nu_\tau \overline{\nu}_e$, hadron$^-$ ν_τ, or $\pi^- \pi^+ \pi^-$ decay modes using classical CL approach of FELDMAN 98.

[58] ESKUT 98 search for events with one μ^- with indication of a kink from τ^- decay in the nuclear emulsion. No candidates were found in a 31,423 event subsample.

[59] ESKUT 98B search for $\tau^- \to \mu^- \nu_\tau \overline{\nu}_\mu$ or $h^- \nu_\tau \overline{\nu}_\mu$, where h^- is a negatively charged hadron. The μ^- sample is somewhat larger than in ESKUT 98, which this result supersedes. Bayesian limit.

[60] LOVERRE 96 uses the charged-current to neutral-current ratio from the combined CHARM (ALLABY 86) and CDHS (ABRAMOWICZ 86) data from 1986.

$\overline{\nu}_\mu \to \overline{\nu}_\tau$

$\Delta(m^2)$ for $\sin^2(2\theta) = 1$

VALUE (eV^2)	CL%	DOCUMENT ID		TECN	COMMENT
<2.2	90	ASRATYAN	81	HLBC	FNAL
• • • We do not use the following data for averages, fits, limits, etc. • • •					
<1.4	90	MCFARLAND	95	CCFR	FNAL
<6.5	90	BOFILL	87	CNTR	FNAL
<7.4	90	TAYLOR	83	HLBC	15-ft FNAL

$\sin^2(2\theta)$ for "Large" $\Delta(m^2)$

VALUE	CL%	DOCUMENT ID		TECN	COMMENT
<4.4 $\times 10^{-2}$	90	ASRATYAN	81	HLBC	FNAL
• • • We do not use the following data for averages, fits, limits, etc. • • •					
<0.0081	90	MCFARLAND	95	CCFR	FNAL
<0.15	90	BOFILL	87	CNTR	FNAL
<8.8 $\times 10^{-2}$	90	TAYLOR	83	HLBC	15-ft FNAL

$\nu_\mu(\overline{\nu}_\mu) \rightarrow \nu_\tau(\overline{\nu}_\tau)$

$\Delta(m^2)$ for $\sin^2(2\theta) = 1$

VALUE (eV^2)	CL%	DOCUMENT ID		TECN	COMMENT
<1.5	90	[61] GRUWE	93	CHM2	CERN SPS

[61] GRUWE 93 is a search using the CHARM II detector in the CERN SPS wide-band neutrino beam for $\nu_\mu \rightarrow \nu_\tau$ and $\overline{\nu}_\mu \rightarrow \overline{\nu}_\tau$ oscillations signalled by quasi-elastic ν_τ and $\overline{\nu}_\tau$ interactions followed by the decay $\tau \rightarrow \nu_\tau \pi$. The maximum sensitivity in $\sin^2 2\theta$ ($< 6.4 \times 10^{-3}$ at the 90% CL) is reached for $\Delta(m^2) \simeq 50$ eV^2.

$\sin^2(2\theta)$ for "Large" $\Delta(m^2)$

VALUE (units 10^{-3})	CL%	DOCUMENT ID		TECN	COMMENT
<8	90	[62] GRUWE	93	CHM2	CERN SPS

[62] GRUWE 93 is a search using the CHARM II detector in the CERN SPS wide-band neutrino beam for $\nu_\mu \rightarrow \nu_\tau$ and $\overline{\nu}_\mu \rightarrow \overline{\nu}_\tau$ oscillations signalled by quasi-elastic ν_τ and $\overline{\nu}_\tau$ interactions followed by the decay $\tau \rightarrow \nu_\tau \pi$. The maximum sensitivity in $\sin^2 2\theta$ ($< 6.4 \times 10^{-3}$ at the 90% CL) is reached for $\Delta(m^2) \simeq 50$ eV^2.

$\nu_\mu \not\rightarrow \nu_\mu$

$\Delta(m^2)$ for $\sin^2(2\theta) = 1$

VALUE (eV^2)	CL%	DOCUMENT ID		TECN	COMMENT
>0.0015 AND < 0.0039	90	[63] AHN	03	K2K	KEK to Super-K
• • • We do not use the following data for averages, fits, limits, etc. • • •					
< 0.29 OR >22	90	BERGSMA	88	CHRM	
<7	90	BELIKOV	85	CNTR	Serpukhov
<8.0 OR >1250	90	STOCKDALE	85	CNTR	
<0.29 OR >22	90	BERGSMA	84	CHRM	
<0.23 OR >100	90	DYDAK	84	CNTR	
<13 OR >1500	90	STOCKDALE	84	CNTR	
<8.0	90	BELIKOV	83	CNTR	

[63] K2K is a 250 km long-baseline disappearance experiment. The result indicates neutrino oscillations. The measured oscillation parameters are consistent with the ones suggested by atmospheric neutrino observations.

$\sin^2(2\theta)$ for $\Delta(m^2) = 0.003$ eV^2

VALUE	CL%	DOCUMENT ID		TECN	COMMENT
• • • We do not use the following data for averages, fits, limits, etc. • • •					
> 0.35	90	[64] AHN	03	K2K	KEK to Super-K

[64] K2K is a 250 km long-baseline disappearance experiment. The result indicates neutrino oscillations. The measured oscillation parameters are consistent with the ones suggested by atmospheric neutrino observations.

$\sin^2(2\theta)$ for $\Delta(m^2) = 100\text{eV}^2$

VALUE	CL%	DOCUMENT ID		TECN	COMMENT
<0.02	90	[65] STOCKDALE	85	CNTR	FNAL
• • • We do not use the following data for averages, fits, limits, etc. • • •					
<0.17	90	[66] BERGSMA	88	CHRM	
<0.07	90	[67] BELIKOV	85	CNTR	Serpukhov
<0.27	90	[66] BERGSMA	84	CHRM	CERN PS
<0.1	90	[68] DYDAK	84	CNTR	CERN PS
<0.02	90	[69] STOCKDALE	84	CNTR	FNAL
<0.1	90	[70] BELIKOV	83	CNTR	Serpukhov

[65] This bound applies for $\Delta(m^2) = 100$ eV^2. Less stringent bounds apply for other $\Delta(m^2)$; these are nontrivial for $8 < \Delta(m^2) <1250$ eV^2.

[66] This bound applies for $\Delta(m^2) = 0.7$–9. eV^2. Less stringent bounds apply for other $\Delta(m^2)$; these are nontrivial for $0.28 < \Delta(m^2) <22$ eV^2.

[67] This bound applies for a wide range of $\Delta(m^2) >7$ eV^2. For some values of $\Delta(m^2)$, the value is less stringent; the least restrictive, nontrivial bound occurs approximately at $\Delta(m^2) = 300$ eV^2 where $\sin^2(2\theta) <0.13$ at CL = 90%.

[68] This bound applies for $\Delta(m^2) = 1.$–10. eV^2. Less stringent bounds apply for other $\Delta(m^2)$; these are nontrivial for $0.23 < \Delta(m^2) <90$ eV^2.

[69] This bound applies for $\Delta(m^2) = 110$ eV^2. Less stringent bounds apply for other $\Delta(m^2)$; these are nontrivial for $13 < \Delta(m^2) <1500$ eV^2.

[70] Bound holds for $\Delta(m^2) = 20$–1000 eV^2.

$\overline{\nu}_\mu \not\to \overline{\nu}_\mu$

$\Delta(m^2)$ for $\sin^2(2\theta) = 1$

VALUE (eV^2)	CL%	DOCUMENT ID		TECN
<7 OR >1200 OUR LIMIT				
<7 OR >1200	90	STOCKDALE	85	CNTR

$\sin^2(2\theta)$ for 190 eV^2 < $\Delta(m^2)$ < 320 eV^2

VALUE	CL%	DOCUMENT ID		TECN	COMMENT
<0.02	90	[71] STOCKDALE	85	CNTR	FNAL

[71] This bound applies for $\Delta(m^2)$ between 190 and 320 or = 530 eV^2. Less stringent bounds apply for other $\Delta(m^2)$; these are nontrivial for $7 < \Delta(m^2) <1200$ eV^2.

$\nu_\mu \to (\overline{\nu}_e)_L$

See note above for $\nu_e \to (\overline{\nu}_e)_L$ limit

$\alpha\Delta(m^2)$ for $\sin^2(2\theta) = 1$

VALUE (eV^2)	CL%	DOCUMENT ID		TECN	COMMENT
<0.16	90	[72] FREEDMAN	93	CNTR	LAMPF
• • • We do not use the following data for averages, fits, limits, etc. • • •					
<0.7	90	[73] COOPER	82	HLBC	BEBC CERN SPS

[72] FREEDMAN 93 is a search at LAMPF for $\overline{\nu}_e$ generated from any of the three neutrino types ν_μ, $\overline{\nu}_\mu$, and ν_e which come from the beam stop. The $\overline{\nu}_e$'s would be detected by the reaction $\overline{\nu}_e p \to e^+ n$. The limit on $\Delta(m^2)$ is better than the CERN BEBC experiment, but the limit on $\sin^2\theta$ is almost a factor of 100 less sensitive.

[73] COOPER 82 states that existing bounds on V+A currents require α to be small.

$\alpha^2\sin^2(2\theta)$ for "Large" $\Delta(m^2)$

VALUE	CL%	DOCUMENT ID		TECN	COMMENT
<0.001	90	[74] COOPER	82	HLBC	BEBC CERN SPS
• • • We do not use the following data for averages, fits, limits, etc. • • •					
<0.07	90	[75] FREEDMAN	93	CNTR	LAMPF

[74] COOPER 82 states that existing bounds on V+A currents require α to be small.

[75] FREEDMAN 93 is a search at LAMPF for $\overline{\nu}_e$ generated from any of the three neutrino types ν_μ, $\overline{\nu}_\mu$, and ν_e which come from the beam stop. The $\overline{\nu}_e$'s would be detected by the reaction $\overline{\nu}_e p \rightarrow e^+ n$. The limit on $\Delta(m^2)$ is better than the CERN BEBC experiment, but the limit on $\sin^2\theta$

(B) Reactor $\overline{\nu}_e$ disappearance experiments

In most cases, the reaction $\overline{\nu}_e p \rightarrow e^+ n$ is observed at different distances from one or more reactors in a complex.

Events (Observed/Expected) from Reactor $\overline{\nu}_e$ Experiments

VALUE	DOCUMENT ID		TECN	COMMENT
• • • We do not use the following data for averages, fits, limits, etc. • • •				
0.611±0.085±0.041	[76] EGUCHI	03	KLND	Japanese react ∼ 180 km
1.01 ±0.024±0.053	[77] BOEHM	01		Palo Verde react. 0.75–0.89 km
1.04 ±0.03 ±0.08	[78] BOEHM	00C		Palo Verde react. 0.75–0.89 km
1.01 ±0.028±0.027	[79] APOLLONIO	99	CHOZ	Chooz reactors 1 km
0.987±0.006±0.037	[80] GREENWOOD	96		Savannah River, 18.2 m
0.988±0.004±0.05	ACHKAR	95	CNTR	Bugey reactor, 15 m
0.994±0.010±0.05	ACHKAR	95	CNTR	Bugey reactor, 40 m
0.915±0.132±0.05	ACHKAR	95	CNTR	Bugey reactor, 95 m
0.987±0.014±0.027	[81] DECLAIS	94	CNTR	Bugey reactor, 15 m
0.985±0.018±0.034	KUVSHINN...	91	CNTR	Rovno reactor
1.05 ±0.02 ±0.05	VUILLEUMIER	82		Gösgen reactor
0.955±0.035±0.110	[82] KWON	81		$\overline{\nu}_e p \rightarrow e^+ n$
0.89 ±0.15	[82] BOEHM	80		$\overline{\nu}_e p \rightarrow e^+ n$
0.38 ±0.21	[83,84] REINES	80		
0.40 ±0.22	[83,84] REINES	80		

[76] EGUCHI 03 observe reactor neutrino disappearance at ∼ 180 km baseline to various Japanese nuclear power reactors. See the footnote in the following table for further details, and the paper for the inclusion/exclusion plot.

[77] BOEHM 01 search for neutrino oscillations at 0.75 and 0.89 km distance from the Palo Verde reactors.

[78] BOEHM 00C search for neutrino oscillations at 0.75 and 0.89 km distance from the Palo Verde reactors.

[79] APOLLONIO 99, APOLLONIO 98 search for neutrino oscillations at 1.1 km fixed distance from Chooz reactors. They use $\overline{\nu}_e p \rightarrow e^+ n$ in Gd-loaded scintillator target. APOLLONIO 99 supersedes APOLLONIO 98. See also APOLLONIO 03 for detailed description.

[80] GREENWOOD 96 search for neutrino oscillations at 18 m and 24 m from the reactor at Savannah River.

[81] DECLAIS 94 result based on integral measurement of neutrons only. Result is ratio of measured cross section to that expected in standard *V-A* theory. Replaced by ACHKAR 95.

[82] KWON 81 represents an analysis of a larger set of data from the same experiment as BOEHM 80.

[83] REINES 80 involves comparison of neutral- and charged-current reactions $\overline{\nu}_e d \rightarrow n p \overline{\nu}_e$ and $\overline{\nu}_e d \rightarrow n n e^+$ respectively. Combined analysis of reactor $\overline{\nu}_e$ experiments was performed by SILVERMAN 81.

[84] The two REINES 80 values correspond to the calculated $\overline{\nu}_e$ fluxes of AVIGNONE 80 and DAVIS 79 respectively.

$\overline{\nu}_e \not\rightarrow \overline{\nu}_e$

$\Delta(m^2)$ for $\sin^2(2\theta) = 1$

VALUE (eV^2)	CL%	DOCUMENT ID		TECN	COMMENT
>8 $\times 10^{-6}$	95	[85] EGUCHI	03	KLND	Japanese react $\sim$ 180 km
• • • We do not use the following data for averages, fits, limits, etc. • • •					
<0.0011	90	[86] BOEHM	01		Palo Verde react. 0.75–0.89 km
<0.0011	90	[87] BOEHM	00		Palo Verde react. 0.8 km
<0.0007	90	[88] APOLLONIO	99	CHOZ	Chooz reactors 1 km
<0.01	90	[89] ACHKAR	95	CNTR	Bugey reactor
<0.0075	90	[90] VIDYAKIN	94		Krasnoyarsk reactors
<0.04	90	[91] AFONIN	88	CNTR	Rovno reactor
<0.014	68	[92] VIDYAKIN	87		$\overline{\nu}_e p \rightarrow e^+ n$
<0.019	90	[93] ZACEK	86		Gösgen reactor

[85] EGUCHI 03 observe reactor neutrino disappearance at $\sim$ 180 km baseline to various Japanese nuclear power reactors. This is the lower limit on the mass difference spread, unlike all other entries in this table. Observation is consistent with neutrino oscillations, with mass-mixing and mixing-angle parameters in the Large Mixing Angle Solution region of the solar neutrino problem.

[86] BOEHM 01, a continuation of BOEHM 00, is a disappearance search for neutrino oscillations at 0.75 and 0.89 km distance from the Palo Verde reactors. Result is less restrictive than APOLLONIO 99.

[87] BOEHM 00 is a disappearance search for neutrino oscillations at 0.75 and 0.89 km distance from Palo Verde reactors. The detection reaction is $\overline{\nu}_e p \rightarrow e^+ n$ in a segmented Gd loaded scintillator target. Result is less restrictive than APOLLONIO 99.

[88] APOLLONIO 99 search for neutrino oscillations at 1.1 km fixed distance from Chooz reactors. They use $\overline{\nu}_e p \rightarrow e^+ n$ in Gd-loaded scintillator target. APOLLONIO 99 supersedes APOLLONIO 98. This is the most sensitive search in terms of $\Delta(m^2)$ for $\overline{\nu}_e$ disappearance. See also APOLLONIO 03 for detailed description.

[89] ACHKAR 95 bound is for L=15, 40, and 95 m.

[90] VIDYAKIN 94 bound is for L=57.0 m, 57.6 m, and 231.4 m. Supersedes VIDYAKIN 90.

[91] AFONIN 86 and AFONIN 87 also give limits on $\sin^2(2\theta)$ for intermediate values of $\Delta(m^2)$. (See also KETOV 92). Supersedes AFONIN 87, AFONIN 86, AFONIN 85, AFONIN 83, and BELENKII 83.

[92] VIDYAKIN 87 bound is for L = 32.8 and 92.3 m distance from two reactors.

[93] This bound is from data for L=37.9 m, 45.9 m, and 64.7 m.

$\sin^2(2\theta)$ for "Large" $\Delta(m^2)$

VALUE	CL%	DOCUMENT ID		TECN	COMMENT
>0.4	95	[94] EGUCHI	03	KLND	Japanese react $\sim$ 180 km
• • • We do not use the following data for averages, fits, limits, etc. • • •					
<0.17	90	[95] BOEHM	01		Palo Verde react. 0.75–0.89 km
<0.21	90	[96] BOEHM	00		Palo Verde react. 0.8 km
<0.10	90	[97] APOLLONIO	99	CHOZ	Chooz reactors 1 km
<0.24	90	[98] GREENWOOD	96		
<0.04	90	[98] GREENWOOD	96		For $\Delta(m^2) = 1.0$ eV^2
<0.02	90	[99] ACHKAR	95	CNTR	For $\Delta(m^2) = 0.6$ eV^2
<0.087	68	[100] VYRODOV	95	CNTR	For $\Delta(m^2)$ >2 eV^2
<0.15	90	[101] VIDYAKIN	94		For $\Delta(m^2) > 5.0 \times 10^{-2}$ eV^2
<0.2	90	[102] AFONIN	88	CNTR	$\overline{\nu}_e p \rightarrow e^+ n$
<0.14	68	[103] VIDYAKIN	87		$\overline{\nu}_e p \rightarrow e^+ n$
<0.21	90	[104] ZACEK	86		$\overline{\nu}_e p \rightarrow e^+ n$
<0.19	90	[105] ZACEK	85		Gösgen reactor
<0.16	90	[106] GABATHULER	84		$\overline{\nu}_e p \rightarrow e^+ n$

[94] EGUCHI 03 observe reactor neutrino disappearance at $\sim$ 180 km baseline to various Japanese nuclear power reactors. This is the lower limit on $\sin^2 2\theta$, unlike all other entries in this table. It is based on the observed rate only; consideration of the spectrum shape results in somewhat more restrictive limit. Observation is consistent with neutrino oscillations, with mass-mixing and mixing-angle parameters in the Large Mixing Angle Solution region of the solar neutrino problem.

[95] BOEHM 01 search for neutrino oscillations at 0.75 and 0.89 km distance from the Palo Verde reactors. Continuation of BOEHM 00.

[96] BOEHM 00 search for neutrino oscillations at 0.75 and 0.89 km distance from Palo Verde reactors.

[97] APOLLONIO 99 search for neutrino oscillations at 1.1 km fixed distance from Chooz reactors. See also APOLLONIO 03 for detailed description.

[98] GREENWOOD 96 search for neutrino oscillations at 18 m and 24 m from the reactor at Savannah River by observing $\overline{\nu}_e p \rightarrow e^+ n$ in a Gd loaded scintillator target. Their region of sensitivity in $\Delta(m^2)$ and $\sin^2 2\theta$ is already excluded by ACHKAR 95.

[99] ACHKAR 95 bound is from data for L=15, 40, and 95 m distance from the Bugey reactor.

[100] The VYRODOV 95 bound is from data for L=15 m distance from the Bugey-5 reactor.

[101] The VIDYAKIN 94 bound is from data for L=57.0 m, 57.6 m, and 231.4 m from three reactors in the Krasnoyarsk Reactor complex.

[102] Several different methods of data analysis are used in AFONIN 88. We quote the most stringent limits. Different upper limits on $\sin^2 2\theta$ apply at intermediate values of $\Delta(m^2)$. Supersedes AFONIN 87, AFONIN 85, and BELENKII 83.

[103] VIDYAKIN 87 bound is for L = 32.8 and 92.3 m distance from two reactors.

[104] This bound is from data for L=37.9 m, 45.9 m, and 64.7 m distance from Gosgen reactor.

[105] ZACEK 85 gives two sets of bounds depending on what assumptions are used in the data analysis. The bounds in figure 3(a) of ZACEK 85 are progressively poorer for large $\Delta(m^2)$ whereas those of figure 3(b) approach a constant. We list the latter. Both sets of bounds use combination of data from 37.9, 45.9, and 64.7m distance from reactor. ZACEK 85 states "Our experiment excludes this area (the oscillation parameter region allowed by the Bugey data, CAVAIGNAC 84) almost completely, thus disproving the indications of neutrino oscillations of CAVAIGNAC 84 with a high degree of confidence."

[106] This bound comes from a combination of the VUILLEUMIER 82 data at distance 37.9m from Gosgen reactor and new data at 45.9m.

(C) Atmospheric neutrino observations

Neutrinos and antineutrinos produced in the atmosphere induce μ-like and e-like events in underground detectors. The ratio of the numbers of the two kinds of events is defined as μ/e. It has the advantage that systematic effects, such as flux uncertainty, tend to cancel, for both experimental and theoretical values of the ratio. The "ratio of the ratios" of experimental to theoretical μ/e, $R(\mu/e)$, or that of experimental to theoretical μ/total, $R(\mu/\text{total})$ with total $= \mu+e$, is reported below. If the actual value is not unity, the value obtained in a given experiment may depend on the experimental conditions.

R(μ/e) = (Measured Ratio μ/e) / (Expected Ratio μ/e)

VALUE	DOCUMENT ID		TECN	COMMENT
• • • We do not use the following data for averages, fits, limits, etc. • • •				
$0.64 \pm 0.11 \pm 0.06$	[107] ALLISON	99	SOU2	Calorimeter
$0.61 \pm 0.03 \pm 0.05$	[108] FUKUDA	98	SKAM	sub-GeV
$0.66 \pm 0.06 \pm 0.08$	[109] FUKUDA	98E	SKAM	multi-GeV
	[110] FUKUDA	96B	KAMI	Water Cherenkov
$1.00 \pm 0.15 \pm 0.08$	[111] DAUM	95	FREJ	Calorimeter
$0.60 \,^{+0.06}_{-0.05} \pm 0.05$	[112] FUKUDA	94	KAMI	sub-GeV
$0.57 \,^{+0.08}_{-0.07} \pm 0.07$	[113] FUKUDA	94	KAMI	multi-Gev
	[114] BECKER-SZ...	92B	IMB	Water Cherenkov

[107] ALLISON 99 result is based on an exposure of 3.9 kton yr, 2.6 times the exposure reported in ALLISON 97, and replaces that result.

[108] FUKUDA 98 result is based on an exposure of 25.5 kton yr. The analyzed data sample consists of fully-contained e-like events with 0.1 GeV/c<p_e and μ-like events with 0.2 GeV/c<p_μ, both having a visible energy $<$ 1.33 GeV. These criteria match the definition used by FUKUDA 94.

[109] FUKUDA 98E result is based on an exposure of 25.5 kton yr. The analyzed data sample consists of fully-contained single-ring events with visible energy $>$ 1.33 GeV and partially contained events. All partially contained events are classified as μ-like.

[110] FUKUDA 96B studied neutron background in the atmospheric neutrino sample observed in the Kamiokande detector. No evidence for the background contamination was found.

[111] DAUM 95 results are based on an exposure of 2.0 kton yr which includes the data used by BERGER 90B. This ratio is for the contained and semicontained events. DAUM 95 also report $R(\mu/e) = 0.99 \pm 0.13 \pm 0.08$ for the total neutrino induced data sample which includes upward going stopping muons and horizontal muons in addition to the contained and semicontained events.

[112] FUKUDA 94 result is based on an exposure of 7.7 kton yr and updates the HIRATA 92 result. The analyzed data sample consists of fully-contained e-like events with $0.1 < p_e < 1.33$ GeV/c and fully-contained μ-like events with $0.2 < p_\mu < 1.5$ GeV/c.

[113] FUKUDA 94 analyzed the data sample consisting of fully contained events with visible energy $>$ 1.33 GeV and partially contained μ-like events.

[114] BECKER-SZENDY 92B reports the fraction of nonshowering events (mostly muons from atmospheric neutrinos) as $0.36 \pm 0.02 \pm 0.02$, as compared with expected fraction $0.51 \pm 0.01 \pm 0.05$. After cutting the energy range to the Kamiokande limits, BEIER 92 finds $R(\mu/e)$ very close to the Kamiokande value.

R(ν_μ) = (Measured Flux of ν_μ) / (Expected Flux of ν_μ)

VALUE	DOCUMENT ID		TECN	COMMENT
• • • We do not use the following data for averages, fits, limits, etc. • • •				
$0.72 \pm 0.026 \pm 0.13$	[115] AMBROSIO	01	MCRO	upward through-going
$0.57 \pm 0.05 \pm 0.15$	[116] AMBROSIO	00	MCRO	upgoing partially contained
$0.71 \pm 0.05 \pm 0.19$	[117] AMBROSIO	00	MCRO	downgoing partially contained + upgoing stopping
$0.74 \pm 0.036 \pm 0.046$	[118] AMBROSIO	98	MCRO	Streamer tubes
	[119] CASPER	91	IMB	Water Cherenkov
	[120] AGLIETTA	89	NUSX	
0.95 ± 0.22	[121] BOLIEV	81		Baksan
0.62 ± 0.17	CROUCH	78		Case Western/UCI

[115] AMBROSIO 01 result is based on the upward through-going muon tracks with $E_\mu > 1$ GeV. The data came from three different detector configurations, but the statistics is largely dominated by the full detector run, from May 1994 to December 2000. The total live time, normalized to the full detector configuration, is 6.17 years. The first error is the statistical error, the second is the systematic error, dominated by the theoretical error in the predicted flux.

[116] AMBROSIO 00 result is based on the upgoing partially contained event sample. It came from 4.1 live years of data taking with the full detector, from April 1994 to February 1999. The average energy of atmospheric muon neutrinos corresponding to this sample is 4 GeV. The first error is statistical, the second is the systematic error, dominated by the 25% theoretical error in the rate (20% in the flux and 15% in the cross section, added in quadrature). Within statistics, the observed deficit is uniform over the zenith angle.

[117] AMBROSIO 00 result is based on the combined samples of downgoing partially contained events and upgoing stopping events. These two subsamples could not be distinguished due to the lack of timing information. The result came from 4.1 live years of data taking with the full detector, from April 1994 to February 1999. The average energy of atmospheric muon neutrinos corresponding to this sample is 4 GeV. The first error is statistical, the second is the systematic error, dominated by the 25% theoretical error in the rate (20% in the flux and 15% in the cross section, added in quadrature). Within statistics, the observed deficit is uniform over the zenith angle.

[118] AMBROSIO 98 result is for all nadir angles and updates AHLEN 95 result. The lower cutoff on the muon energy is 1 GeV. In addition to the statistical and systematic errors, there is a Monte Carlo flux error (theoretical error) of ± 0.13. With a neutrino oscillation hypothesis, the fit either to the flux or zenith distribution independently yields $\sin^2 2\theta = 1.0$ and $\Delta(m^2) \sim$ a few times 10^{-3} eV^2. However, the fit to the observed zenith distribution gives a maximum probability for χ^2 of only 5% for the best oscillation hypothesis.

[119] CASPER 91 correlates showering/nonshowering signature of single-ring events with parent atmospheric-neutrino flavor. They find nonshowering ($\approx \nu_\mu$ induced) fraction is $0.41 \pm 0.03 \pm 0.02$, as compared with expected 0.51 ± 0.05 (syst).

[120] AGLIETTA 89 finds no evidence for any anomaly in the neutrino flux. They define ρ = (measured number of ν_e's)/(measured number of ν_μ's). They report $\rho(\text{measured}) = \rho(\text{expected}) = 0.96^{+0.32}_{-0.28}$.

[121] From this data BOLIEV 81 obtain the limit $\Delta(m^2) \leq 6 \times 10^{-3}$ eV^2 for maximal mixing, $\nu_\mu \not\rightarrow \nu_\mu$ type oscillation.

R(μ/total) = (Measured Ratio μ/total) / (Expected Ratio μ/total)

VALUE	DOCUMENT ID		TECN	COMMENT
• • • We do not use the following data for averages, fits, limits, etc. • • •				
$1.1^{+0.07}_{-0.12} \pm 0.11$	[122] CLARK	97	IMB	multi-GeV

[122] CLARK 97 obtained this result by an analysis of fully contained and partially contained events in the IMB water-Cherenkov detector with visible energy > 0.95 GeV.

$N_{up}(\mu)/N_{down}(\mu)$

VALUE	DOCUMENT ID	TECN	COMMENT
• • • We do not use the following data for averages, fits, limits, etc. • • •			
$0.52^{+0.07}_{-0.06} \pm 0.01$	[123] FUKUDA	98E SKAM	multi-GeV

[123] FUKUDA 98E result is based on an exposure of 25.5 kton yr. The analyzed data sample consists of fully-contained single-ring μ-like events with visible energy > 1.33 GeV and partially contained events. All partially contained events are classified as μ-like. Upward-going events are those with $-1 <$cos (zenith angle) < -0.2 and downward-going events with those with $0.2 <$cos (zenith angle) < 1. FUKUDA 98E result strongly deviates from an expected value of $0.98 \pm 0.03 \pm 0.02$.

$N_{up}(e)/N_{down}(e)$

VALUE	DOCUMENT ID	TECN	COMMENT
• • • We do not use the following data for averages, fits, limits, etc. • • •			
$0.84^{+0.14}_{-0.12} \pm 0.02$	[124] FUKUDA	98E SKAM	multi-GeV

[124] FUKUDA 98E result is based on an exposure of 25.5 kton yr. The analyzed data sample consists of fully-contained single-ring e-like events with visible energy > 1.33 GeV. Upward-going events are those with $-1 <$cos (zenith angle) < -0.2 and downward-going events are those with $0.2 <$cos (zenith angle) < 1. FUKUDA 98E result is compared to an expected value of $1.01 \pm 0.06 \pm 0.03$.

$\sin^2(2\theta)$ for given $\Delta(m^2)$ ($\nu_e \leftrightarrow \nu_\mu$)

For a review see BAHCALL 89.

VALUE	CL%	DOCUMENT ID	TECN	COMMENT
• • • We do not use the following data for averages, fits, limits, etc. • • •				
<0.6	90	[125] OYAMA	98 KAMI	$\Delta(m^2) > 0.1$ eV^2
<0.5		[126] CLARK	97 IMB	$\Delta(m^2) > 0.1$ eV^2
>0.55	90	[127] FUKUDA	94 KAMI	$\Delta(m^2) = 0.007$–0.08 eV^2
<0.47	90	[128] BERGER	90B FREJ	$\Delta(m^2) > 1$ eV^2
<0.14	90	LOSECCO	87 IMB	$\Delta(m^2) = 0.00011$ eV^2

[125] OYAMA 98 obtained this result by an analysis of upward-going muons in Kamiokande. The data sample used is essentially the same as that used by HATAKEYAMA 98.

[126] CLARK 97 obtained this result by an analysis of fully contained and partially contained events in the IMB water-Cherenkov detector with visible energy > 0.95 GeV.

[127] FUKUDA 94 obtained this result by a combined analysis of sub- and multi-GeV atmospheric neutrino events in Kamiokande.

[128] BERGER 90B uses the Frejus detector to search for oscillations of atmospheric neutrinos. Bounds are for both neutrino and antineutrino oscillations.

$\Delta(m^2)$ for $\sin^2(2\theta) = 1$ ($\nu_e \leftrightarrow \nu_\mu$)

VALUE (10^{-5} eV^2)	CL%	DOCUMENT ID	TECN
• • • We do not use the following data for averages, fits, limits, etc. • • •			
<560	90	[129] OYAMA	98 KAMI
<980		[130] CLARK	97 IMB
$700 < \Delta(m^2) < 7000$	90	[131] FUKUDA	94 KAMI
<150	90	[132] BERGER	90B FREJ

[129] OYAMA 98 obtained this result by an analysis of upward-going muons in Kamiokande. The data sample used is essentially the same as that used by HATAKEYAMA 98.

[130] CLARK 97 obtained this result by an analysis of fully contained and partially contained events in the IMB water-Cherenkov detector with visible energy > 0.95 GeV.

[131] FUKUDA 94 obtained this result by a combined analysis of sub- and multi-GeV atmospheric neutrino events in Kamiokande.

[132] BERGER 90B uses the Frejus detector to search for oscillations of atmospheric neutrinos. Bounds are for both neutrino and antineutrino oscillations.

$\sin^2(2\theta)$ for given $\Delta(m^2)$ ($\overline{\nu}_e \leftrightarrow \overline{\nu}_\mu$)

VALUE (10^{-5} eV^2)	CL%	DOCUMENT ID		TECN	COMMENT
• • • We do not use the following data for averages, fits, limits, etc. • • •					
<0.9	99	[133] SMIRNOV	94	THEO	$\Delta(m^2) > 3\times10^{-4}$ eV^2
<0.7	99	[133] SMIRNOV	94	THEO	$\Delta(m^2) < 10^{-11}$ eV^2

[133] SMIRNOV 94 analyzed the data from SN 1987A using stellar-collapse models. They also give less stringent upper limits on $\sin^2 2\theta$ for $10^{-11} < \Delta(m^2) < 3\times10^{-7}$ eV^2 and $10^{-5} < \Delta(m^2) < 3\times10^{-4}$ eV^2. The same results apply to $\overline{\nu}_e \leftrightarrow \overline{\nu}_\tau$, ν_μ, and ν_τ.

$\sin^2(2\theta)$ for given $\Delta(m^2)$ ($\nu_\mu \leftrightarrow \nu_\tau$)

VALUE	CL%	DOCUMENT ID		TECN	COMMENT
• • • We do not use the following data for averages, fits, limits, etc. • • •					
>0.45	90	[134] AMBROSIO	03	MCRO	$\Delta(m^2)$= 0.00025–0.009 eV^2
>0.77	90	[135] AMBROSIO	03	MCRO	$\Delta(m^2)$= 0.0006–0.007 eV^2
>0.8	90	[136] AMBROSIO	01	MCRO	$\Delta(m^2)$= 0.0006–0.015 eV^2
>0.82	90	[137] AMBROSIO	01	MCRO	$\Delta(m^2)$= 0.001–0.006 ev^2
>0.25	90	[138] AMBROSIO	00	MCRO	$\Delta(m^2) > 3\times10^{-4}$ eV^2
>0.4	90	[139] FUKUDA	99C	SKAM	$\Delta(m^2)$= 0.001–0.1 eV^2
>0.7	90	[140] FUKUDA	99D	SKAM	$\Delta(m^2)$= 0.0015–0.015 eV^2
>0.82	90	[141] AMBROSIO	98	MCRO	$\Delta(m^2) \sim 0.0025$ eV^2
>0.82	90	[142] FUKUDA	98C	SKAM	$\Delta(m^2)$ = 0.0005–0.006 eV^2
>0.3	90	[143] HATAKEYAMA	98	KAMI	$\Delta(m^2)$= 0.00055–0.14 eV^2
>0.73	90	[144] HATAKEYAMA	98	KAMI	$\Delta(m^2)$= 0.004–0.025 eV^2
<0.7		[145] CLARK	97	IMB	$\Delta(m^2) >$ 0.1 eV^2
>0.65	90	[146] FUKUDA	94	KAMI	$\Delta(m^2)$ = 0.005–0.03 eV^2
<0.5	90	[147] BECKER-SZ...	92	IMB	$\Delta(m^2)$= 1–2 $\times10^{-4}$ eV^2
<0.6	90	[148] BERGER	90B	FREJ	$\Delta(m^2) > 1$ eV^2

[134] AMBROSIO 03 obtained this result on the basis of the ratio R=$N_{\rm low}/N_{\rm high}$, where $N_{\rm low}$ and $N_{\rm high}$ are the number of upward through-going muon events with reconstructed neutrino energy <30 GeV and >130 GeV, respectively. The data came from the full detector run started in 1994. The method of FELDMAN 98 is used to obtain the limits.

[135] AMBROSIO 03 obtained this result by using the ratio R and the angular distribution of the upward through-going muons. R is given by $N_{\rm low}/N_{\rm high}$, where $N_{\rm low}$ and $N_{\rm high}$ are the number of events with reconstructed neutrino energy <30 and >130 GeV, respectively. The angular distribution is reported in AMBROSIO 01. The method of FELDMAN 98 is used to obtain the limits.

[136] AMBROSIO 01 result is based on the angular distribution of upward through-going muon tracks with $E_\mu > 1$ GeV. The data came from three different detector configurations, but the statistics is largely dominated by the full detector run, from May 1994 to December 2000. The total live time, normalized to the full detector configuration, is 6.17 years.

The best fit is obtained outside the physical region. The method of FELDMAN 98 is used to obtain the limits.

[137] AMBROSIO 01 result is based on the angular distribution and normalization of upward through-going muon tracks with $E_\mu > 1$ GeV. The best fit is obtained outside the physical region. The method of FELDMAN 98 is used to obtain the limits. See the previous footnote.

[138] AMBROSIO 00 obtained this result by using the upgoing partially contained event sample and the combined samples of downgoing partially contained events and upgoing stopping events. These data came from 4.1 live years of data taking with the full detector, from April 1994 to February 1999. The average energy of atmospheric muon neutrinos corresponding to these samples is 4 GeV. The maximum of the χ^2 probability (97%) occurs at maximal mixing and $\Delta(m^2)=(1\sim 20)\times 10^{-3}$ eV^2.

[139] FUKUDA 99C obtained this result from a total of 537 live days of upward through-going muon data in Super-Kamiokande between April 1996 to January 1998. With a threshold of $E_\mu > 1.6$ GeV, the observed flux of upward through-going muons is $(1.74 \pm 0.07 \pm 0.02)\times 10^{-13}$ cm^{-2} s^{-1} sr^{-1}. The zenith-angle dependence of the flux does not agree with no-oscillation predictions. For the $\nu_\mu \rightarrow \nu_\tau$ hypothesis, FUKUDA 99C obtained the best fit at $\sin^2 2\theta$=0.95 and $\Delta(m^2)=5.9\times 10^{-3}$ eV^2. FUKUDA 99C also reports 68% and 99% confidence-level allowed regions for the same hypothesis.

[140] FUKUDA 99D obtained this result from a simultaneous fitting to zenith angle distributions of upward-stopping and through-going muons. The flux of upward-stopping muons of minimum energy of 1.6 GeV measured between April 1996 and January 1998 is $(0.39 \pm 0.04 \pm 0.02)\times 10^{-13}$ cm^{-2} s^{-1} sr^{-1}. This is compared to the expected flux of $(0.73 \pm 0.16$ (theoretical error)$)\times 10^{-13}$ cm^{-2} s^{-1} sr^{-1}. The flux of upward through-going muons is taken from FUKUDA 99C. For the $\nu_\mu \rightarrow \nu_\tau$ hypothesis, FUKUDA 99D obtained the best fit in the physical region at $\sin^2 2\theta$=1.0 and $\Delta(m^2)=3.9\times 10^{-3}$ eV^2. FUKUDA 99D also reports 68% and 99% confidence-level allowed regions for the same hypothesis. FUKUDA 99D further reports the result of the oscillation analysis using the zenith-angle dependence of upward-stopping/through-going flux ratio. The best fit in the physical region is obtained at $\sin^2 2\theta$=1.0 and $\Delta(m^2)=3.1\times 10^{-3}$ eV^2.

[141] AMBROSIO 98 result is only 17% probable at maximum because of relatively low flux for $\cos\theta < -0.8$.

[142] FUKUDA 98C obtained this result by an analysis of 33.0 kton yr atmospheric-neutrino data which include the 25.5 kton yr data used by FUKUDA 98 (sub-GeV) and FUKUDA 98E (multi-GeV). Inside the physical region, the best fit was obtained at $\sin^2 2\theta$=1.0 and $\Delta(m^2)=2.2\times 10^{-3}$ eV^2. In addition, FUKUDA 98C gave the 99% confidence interval, $\sin^2 2\theta > 0.73$ and $3\times 10^{-4} < \Delta(m^2) < 8.5\times 10^{-3}$ eV^2. FUKUDA 98C also tested the $\nu_\mu \rightarrow \nu_e$ hypothesis, and concluded that it is not favored.

[143] HATAKEYAMA 98 obtained this result from a total of 2456 live days of upward-going muon data in Kamiokande between December 1985 and May 1995. With a threshold of $E_\mu > 1.6$ GeV, the observed flux of upward through-going muon is $(1.94 \pm 0.10^{+0.07}_{-0.06})\times 10^{-13}$ cm^{-2} s^{-1} sr^{-1}. This is compared to the expected flux of $(2.46 \pm 0.54$ (theoretical error)$)\times 10^{-13}$ cm^{-2} s^{-1} sr^{-1}. For the $\nu_\mu \rightarrow \nu_\tau$ hypothesis, the best fit inside the physical region was obtained at $\sin^2 2\theta$=1.0 and $\Delta(m^2)=3.2\times 10^{-3}$ eV^2.

[144] HATAKEYAMA 98 obtained this result from a combined analysis of Kamiokande's contained events (FUKUDA 94) and upward-going muon events. The best fit was obtained at $\sin^2 2\theta$=0.95 and $\Delta(m^2)=1.3\times 10^{-2}$ eV^2.

[145] CLARK 97 obtained this result by an analysis of fully contained and partially contained events in the IMB water-Cherenkov detector with visible energy > 0.95 GeV.

[146] FUKUDA 94 obtained this result by a combined analysis of sub-and multi-GeV atmospheric neutrino events in Kamiokande.

[147] BECKER-SZENDY 92 uses upward-going muons to search for atmospheric ν_μ oscillations. The fraction of muons which stop in the detector is used to search for deviations in the expected spectrum. No evidence for oscillations is found.

[148] BERGER 90B uses the Frejus detector to search for oscillations of atmospheric neutrinos. Bounds are for both neutrino and antineutrino oscillations.

$\Delta(m^2)$ for $\sin^2(2\theta) = 1$ ($\nu_\mu \leftrightarrow \nu_\tau$)

VALUE (10^{-5} eV^2)	CL%	DOCUMENT ID		TECN
• • • We do not use the following data for averages, fits, limits, etc. • • •				
$25 < \Delta(m^2) < 900$	90	[149] AMBROSIO	03	MCRO
$60 < \Delta(m^2) < 700$	90	[150] AMBROSIO	03	MCRO
$60 < \Delta(m^2) < 1500$	90	[151] AMBROSIO	01	MCRO
$100 < \Delta(m^2) < 600$	90	[152] AMBROSIO	01	MCRO
> 35	90	[153] AMBROSIO	00	MCRO
$100 < \Delta(m^2) < 5000$	90	[154] FUKUDA	99C	SKAM
$150 < \Delta(m^2) < 1500$	90	[155] FUKUDA	99D	SKAM
$50 < \Delta(m^2) < 600$	90	[156] AMBROSIO	98	MCRO
$50 < \Delta(m^2) < 600$	90	[157] FUKUDA	98C	SKAM
$55 < \Delta(m^2) < 5000$	90	[158] HATAKEYAMA	98	KAMI
$400 < \Delta(m^2) < 2300$	90	[159] HATAKEYAMA	98	KAMI
< 1500		[160] CLARK	97	IMB
$500 < \Delta(m^2) < 2500$	90	[161] FUKUDA	94	KAMI
< 350	90	[162] BERGER	90B	FREJ

[149] AMBROSIO 03 obtained this result on the basis of the ratio $R = N_{\rm low}/N_{\rm high}$, where $N_{\rm low}$ and $N_{\rm high}$ are the number of upward through-going muon events with reconstructed neutrino energy <30 GeV and >130 GeV, respectively. The data came from the full detector run started in 1994. The method of FELDMAN 98 is used to obtain the limits.

[150] AMBROSIO 03 obtained this result by using the ratio R and the angular distribution of the upward through-going muons. R is given by $N_{\rm low}/N_{\rm high}$, where $N_{\rm low}$ and $N_{\rm high}$ are the number of events with reconstructed neutrino energy <30 and >130 GeV, respectively. The angular distribution is reported in AMBROSIO 01. The method of FELDMAN 98 is used to obtain the limits.

[151] AMBROSIO 01 result is based on the angular distribution of upward through-going muon tracks with $E_\mu > 1$ GeV. The data came from three different detector configurations, but the statistics is largely dominated by the full detector run, from May 1994 to December 2000. The total live time, normalized to the full detector configuration, is 6.17 years. The best fit is obtained outside the physical region. The method of FELDMAN 98 is used to obtain the limits.

[152] AMBROSIO 01 result is based on the angular distribution and normalization of upward through-going muon tracks with $E_\mu > 1$ GeV. The best fit is obtained outside the physical region. The method of FELDMAN 98 is used to obtain the limits. See the previous footnote.

[153] AMBROSIO 00 obtained this result by using the upgoing partially contained event sample and the combined samples of downgoing partially contained events and upgoing stopping events. These data came from 4.1 live years of data taking with the full detector, from April 1994 to February 1999. The average energy of atmospheric muon neutrinos corresponding to these samples is 4 GeV. The maximum of the χ^2 probability (97%) occurs at maximal mixing and $\Delta(m^2) = (1 \sim 20) \times 10^{-3}$ eV^2.

[154] FUKUDA 99C obtained this result from a total of 537 live days of upward through-going muon data in Super-Kamiokande between April 1996 to January 1998. With a threshold of $E_\mu > 1.6$ GeV, the observed flux of upward through-going muon is $(1.74 \pm 0.07 \pm 0.02) \times 10^{-13}$ cm^{-2} s^{-1} sr^{-1}. The zenith-angle dependence of the flux does not agree

with no-oscillation predictions. For the $\nu_\mu \rightarrow \nu_\tau$ hypothesis, FUKUDA 99C obtained the best fit at $\sin^2 2\theta$=0.95 and $\Delta(m^2)$=5.9×10^{-3} eV^2. FUKUDA 99C also reports 68% and 99% confidence-level allowed regions for the same hypothesis.

[155] FUKUDA 99D obtained this result from a simultaneous fitting to zenith angle distributions of upward-stopping and through-going muons. The flux of upward-stopping muons of minimum energy of 1.6 GeV measured between April 1996 and January 1998 is $(0.39 \pm 0.04 \pm 0.02) \times 10^{-13}$ cm^{-2} s^{-1} sr^{-1}. This is compared to the expected flux of $(0.73 \pm 0.16$ (theoretical error)$) \times 10^{-13}$ cm^{-2} s^{-1} sr^{-1}. The flux of upward through-going muons is taken from FUKUDA 99C. For the $\nu_\mu \rightarrow \nu_\tau$ hypothesis, FUKUDA 99D obtained the best fit in the physical region at $\sin^2 2\theta$=1.0 and $\Delta(m^2)$=3.9×10^{-3} eV^2. FUKUDA 99D also reports 68% and 99% confidence-level allowed regions for the same hypothesis. FUKUDA 99D further reports the result of the oscillation analysis using the zenith-angle dependence of upward-stopping/through-going flux ratio. The best fit in the physical region is obtained at $\sin^2 2\theta$=1.0 and $\Delta(m^2)$=3.1×10^{-3} eV^2.

[156] AMBROSIO 98 result is only 17% probable at maximum because of relatively low flux for $\cos\theta < -0.8$.

[157] FUKUDA 98C obtained this result by an analysis of 33.0 kton yr atmospheric-neutrino data which include the 25.5 kton yr data used by FUKUDA 98 (sub-GeV) and FUKUDA 98E (multi-GeV). Inside the physical region, the best fit was obtained at $\sin^2 2\theta$=1.0 and $\Delta(m^2)$=2.2×10^{-3} eV^2. In addition, FUKUDA 98C gave the 99% confidence interval, $\sin^2 2\theta > 0.73$ and $3 \times 10^{-4} < \Delta(m^2) < 8.5 \times 10^{-3}$ eV^2. FUKUDA 98C also tested the $\nu_\mu \rightarrow \nu_e$ hypothesis, and concluded that it is not favored.

[158] HATAKEYAMA 98 obtained this result from a total of 2456 live days of upward-going muon data in Kamiokande between December 1985 and May 1995. With a threshold of $E_\mu > 1.6$ GeV, the observed flux of upward through-going muon is $(1.94 \pm 0.10^{+0.07}_{-0.06}) \times 10^{-13}$ cm^{-2} s^{-1} sr^{-1}. This is compared to the expected flux of $(2.46 \pm 0.54$ (theoretical error)$) \times 10^{-13}$ cm^{-2} s^{-1} sr^{-1}. For the $\nu_\mu \rightarrow \nu_\tau$ hypothesis, the best fit inside the physical region was obtained at $\sin^2 2\theta$=1.0 and $\Delta(m^2)$=3.2×10^{-3} eV^2.

[159] HATAKEYAMA 98 obtained this result from a combined analysis of Kamiokande's contained events (FUKUDA 94) and upward-going muon events. The best fit was obtained at $\sin^2 2\theta$=0.95 and $\Delta(m^2)$=1.3×10^{-2} eV^2.

[160] CLARK 97 obtained this result by an analysis of fully contained and partially contained events in the IMB water-Cherenkov detector with visible energy > 0.95 GeV.

[161] FUKUDA 94 obtained this result by a combined analysis of sub-and multi-GeV atmospheric neutrino events in Kamiokande.

[162] BERGER 90B uses the Frejus detector to search for oscillations of atmospheric neutrinos. Bounds are for both neutrino and antineutrino oscillations.

$\Delta(m^2)$ for $\sin^2(2\theta) = 1$ ($\nu_\mu \rightarrow \nu_s$)

ν_s means ν_τ or any sterile (noninteracting) ν.

VALUE (10^{-5} eV^2)	CL%	DOCUMENT ID		TECN	COMMENT
• • • We do not use the following data for averages, fits, limits, etc. • • •					
<3000 (or <550)	90	[163] OYAMA	89	KAMI	Water Cherenkov
< 4.2 or > 54.	90	BIONTA	88	IMB	Flux has ν_μ, $\overline{\nu}_\mu$, ν_e, and $\overline{\nu}_e$

[163] OYAMA 89 gives a range of limits, depending on assumptions in their analysis. They argue that the region $\Delta(m^2) = (100\text{–}1000) \times 10^{-5}$ eV^2 is not ruled out by any data for large mixing.

Search for $\nu_\mu \rightarrow \nu_s$

VALUE	DOCUMENT ID		TECN	COMMENT
• • • We do not use the following data for averages, fits, limits, etc. • • •				
	[164] AMBROSIO	01	MCRO	matter effects
	[165] FUKUDA	00	SKAM	neutral currents + matter effects

[164] AMBROSIO 01 tested the pure 2-flavor $\nu_\mu \rightarrow \nu_s$ hypothesis using matter effects which change the shape of the zenith-angle distribution of upward through-going muons. With maximum mixing and $\Delta(m^2)$ around 0.0024 eV^2, the $\nu_\mu \rightarrow \nu_s$ oscillation is disfavored with 99% confidence level with respect to the $\nu_\mu \rightarrow \nu_\tau$ hypothesis.

[165] FUKUDA 00 tested the pure 2-flavor $\nu_\mu \rightarrow \nu_s$ hypothesis using three complementary atmospheric-neutrino data samples. With this hypothesis, zenith-angle distributions are expected to show characteristic behavior due to neutral currents and matter effects. In the $\Delta(m^2)$ and $\sin^2 2\theta$ region preferred by the Super-Kamiokande data, the $\nu_\mu \rightarrow \nu_s$ hypothesis is rejected at the 99% confidence level, while the $\nu_\mu \rightarrow \nu_\tau$ hypothesis consistently fits all of the data sample.

(D) Solar ν Experiments

SOLAR NEUTRINOS

Revised November 2003 by K. Nakamura (KEK, High Energy Accelerator Research Organization, Japan).

1. Introduction

The Sun is a main-sequence star at a stage of stable hydrogen burning. It produces an intense flux of electron neutrinos as a consequence of nuclear fusion reactions whose combined effect is

$$4p \rightarrow {}^4\mathrm{He} + 2e^+ + 2\nu_e. \qquad (1)$$

Positrons annihilate with electrons. Therefore, when considering the solar thermal energy generation, a relevant expression is

$$4p + 2e^- \rightarrow {}^4\mathrm{He} + 2\nu_e + 26.73\ \mathrm{MeV} - E_\nu\ , \qquad (2)$$

where E_ν represents the energy taken away by neutrinos, with an average value being $\langle E_\nu \rangle \sim 0.6$ MeV. The neutrino-producing reactions which are at work inside the Sun are enumerated in the first column in Table 1. The second column

in Table 1 shows abbreviation of these reactions. The energy spectrum of each reaction is shown in Fig. 1.

Observation of solar neutrinos directly addresses the theory of stellar structure and evolution, which is the basis of the standard solar model (SSM). The Sun as a well-defined neutrino source also provides extremely important opportunities to investigate nontrivial neutrino properties such as nonzero mass and mixing, because of the wide range of matter density and the great distance from the Sun to the Earth.

A pioneering solar neutrino experiment by Davis and collaborators using ^{37}Cl started in the late 1960's. From the very beginning of the solar-neutrino observation [1], it was recognized that the observed flux was significantly smaller than the SSM prediction, provided nothing happens to the electron neutrinos after they are created in the solar interior. This deficit has been called "the solar-neutrino problem."

In spite of the challenges by the chlorine and gallium radiochemical experiments (GALLEX, SAGE, and GNO) and water-Cherenkov experiments (Kamiokande and Super-Kamiokande), the solar-neutrino problem had persisted for more than 30 years. However, there have been remarkable developments in the past few years and now the solar-neutrino problem has been finally solved.

In 2001, the initial result from SNO (Sudbury Neutrino Observatory) [2], a water Cherenkov detector with heavy water, on the solar-neutrino flux measured via charged-current (CC) reaction, $\nu_e d \to e^- pp$, combined with the Super-Kamiokande's high-statistics flux measurement via νe elastic scattering [3], provided direct evidence for flavor conversion of solar neutrinos [2]. Later in 2002, SNO's measurement of the neutral-current (NC) rate, $\nu d \to \nu pn$, and the updated CC result further strengthened this conclusion [4].

The most probable explanation which can also solve the solar-neutrino problem is neutrino oscillation. At this stage, the LMA (large mixing angle) solution was the most promising. However, at 3σ confidence level, LOW (low probability or low mass) and/or VAC (vacuum) solutions were allowed depending on the method of analysis (see Sec. 3.6). LMA and LOW are solutions of neutrino oscillation in matter [5,6] and VAC is a solution of neutrino oscillation in vacuum. Subsequently, experiments have excluded vacuum oscillations and there exists strong evidence that matter effects are required in the solution to the solar-neutrino problem.

In December 2002, KamLAND (Kamioka Liquid Scintillator Anti-Neutrino Detector), a terrestrial $\bar{\nu}_e$ disappearance experiment using reactor neutrinos, observed clear evidence of neutrino oscillation with the allowed parameter region overlapping with the parameter region of the LMA solution [7]. Assuming CPT invariance, this result directly implies that the true solution of the solar ν_e oscillation has been determined to be LMA. A combined analysis of all the solar-neutrino data and KamLAND data significantly constrained the allowed parameter region. Inside the LMA region, the allowed region splits into two bands with higher Δm^2 and lower Δm^2.

More recently, in September, 2003, SNO reported [8] results on solar-neutrino fluxes observed with NaCl added in heavy water: this improved the sensitivity for the detection of the NC reaction. A global analysis of all the solar neutrino data combined with the KamLAND data further reduced the allowed region to the lower Δm^2 band with the best fit point of $\Delta m^2 = 7.1 \times 10^{-5}$ eV^2 and $\theta = 32.5$ degrees [8].

2. Solar Model Predictions

A standard solar model is based on the standard theory of stellar evolution. A variety of input information is needed in the evolutionary calculations. The most elaborate SSM, BP2000 [9], is presented by Bahcall *et al.* who define their SSM as the solar model which is constructed with the best available physics and input data. Though they used no helioseismological constraints in defining the SSM, the calculated sound speed as a function of the solar radius shows an excellent agreement with the helioseismologically determined sound speed to a precision of 0.1% rms throughout essentially the entire Sun. This greatly strengthens the confidence in the solar model. The BP2000 predictions [9] for the flux and contributions to the event rates in chlorine and gallium solar-neutrino experiments from each neutrino-producing reaction are listed in Table 1. The solar-neutrino spectra shown in Fig. 1 also resulted from the BP2000 calculations [9].

Other recent solar-model predictions for solar-neutrino fluxes were given by Turck-Chieze *et al.* [10] Their model is based on the standard theory of stellar evolution where the best physics available is adopted, but some fundamental inputs such as the *pp* reaction rate and the heavy-element abundance in the Sun are seismically adjusted within the commonly estimated errors aiming at reducing the residual differences between the helioseismologically-determined and the model-calculated sound speeds. Their predictions for the event rates in chlorine and gallium solar-neutrino experiments as well as ^{8}B solar-neutrino flux are shown in the last line in Table 2, where the BP2000 predictions [9] are also shown in the same format. As is apparent from this table, the predictions of the two models are remarkably consistent.

The SSM predicted ^{8}B solar-neutrino flux is proportional to the low-energy cross section factor $S_{17}(0)$ for the ^{7}Be(p,γ)^{8}B

reaction. The BP2000 [9] and Turck-Chieze *et al.* [10] models adopted $S_{17}(0) = 19^{+4}_{-2}$ eV·b. Inspired by the recent precise measurement of the low-energy cross section for the ^{7}Be(p,γ)^{8}B reaction by Junghans *et al.* [11], Bahcall *et al.* [12] calculated the (BP2000 + New ^{8}B) SSM predictions using $S_{17}(0) = (22.3 \pm 0.9)$ eV·b. The results are: a ^{8}B solar-neutrino flux of $5.93(1.00^{+0.14}_{-0.15}) \times 10^6$ cm^{-2} s^{-1}, a chlorine capture rate of $8.59^{+1.1}_{-1.2}$ SNU, and a gallium capture rate of 130^{+9}_{-7} SNU.

Table 1: Neutrino-producing reactions in the Sun (first column) and their abbreviations (second column). The neutrino fluxes and event rates in chlorine and gallium solar-neutrino experiments predicted by Bahcall, Pinsonneault and Basu [9] are listed in the third, fourth, and fifth columns respectively.

		BP2000 [9]		
Reaction	Abbr.	Flux (cm^{-2} s^{-1})	Cl (SNU*)	Ga (SNU*)
$pp \to d\,e^+\,\nu$	*pp*	$5.95(1.00^{+0.01}_{-0.01}) \times 10^{10}$	—	69.7
$pe^-p \to d\,\nu$	*pep*	$1.40(1.00^{+0.015}_{-0.015}) \times 10^8$	0.22	2.8
^{3}He $p \to {}^4$He $e^+\nu$	*hep*	9.3×10^3	0.04	0.1
^{7}Be $e^- \to {}^7$Li $\nu + (\gamma)$	^{7}Be	$4.77(1.00^{+0.10}_{-0.10}) \times 10^9$	1.15	34.2
^{8}B $\to {}^8$Be* $e^+\nu$	^{8}B	$5.05(1.00^{+0.20}_{-0.16}) \times 10^6$	5.76	12.1
^{13}N $\to {}^{13}$C $e^+\nu$	^{13}N	$5.48(1.00^{+0.21}_{-0.17}) \times 10^8$	0.09	3.4
^{15}O $\to {}^{15}$N $e^+\nu$	^{15}O	$4.80(1.00^{+0.25}_{-0.19}) \times 10^8$	0.33	5.5
^{17}F $\to {}^{17}$O $e^+\nu$	^{17}F	$5.63(1.00^{+0.25}_{-0.25}) \times 10^6$	0.0	0.1
Total			$7.6^{+1.3}_{-1.1}$	128^{+9}_{-7}

* 1 SNU (Solar Neutrino Unit) = 10^{-36} captures per atom per second.

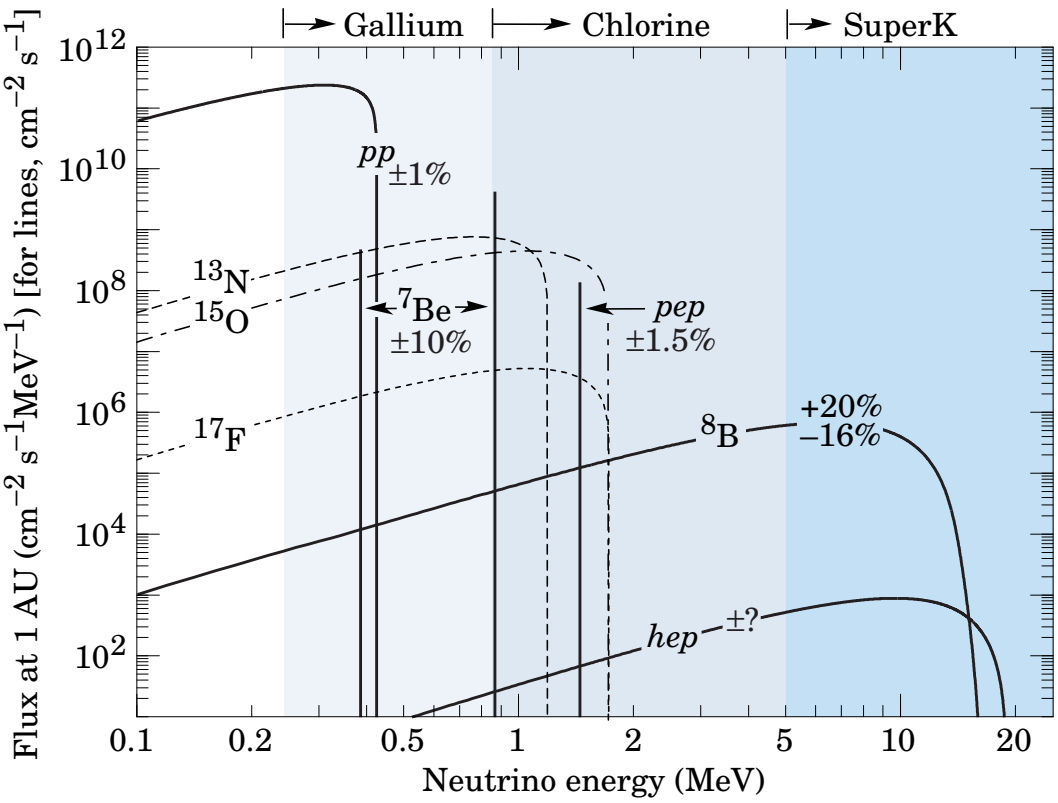

Figure 1: The solar neutrino spectrum predicted by the standard solar model. The neutrino fluxes from continuum sources are given in units of number $\mathrm{cm}^{-2}\mathrm{s}^{-1}\mathrm{MeV}^{-1}$ at one astronomical unit, and the line fluxes are given in number $\mathrm{cm}^{-2}\mathrm{s}^{-1}$. Spectra for the *pp* chain, shown by the solid curves, are courtesy of J.N. Bahcall (2001). Spectra for the CNO chain are shown by the dotted curves, and are also courtesy of J.N. Bahcall (1995). See full-color version on color pages at end of book.

3. Solar Neutrino Experiments

So far, seven solar-neutrino experiments have published results. The most recent published results on the average event

Table 2: Recent results from the seven solar-neutrino experiments and a comparison with standard solar-model predictions. Solar model calculations are also presented. The first and the second errors in the experimental results are the statistical and systematic errors, respectively.

	$^{37}\mathrm{Cl}\rightarrow{}^{37}\mathrm{Ar}$ (SNU)	$^{71}\mathrm{Ga}\rightarrow{}^{71}\mathrm{Ge}$ (SNU)	$^{8}\mathrm{B}$ ν flux ($10^{6}\mathrm{cm}^{-2}\mathrm{s}^{-1}$)
Homestake			
(CLEVELAND 98)[13]	$2.56 \pm 0.16 \pm 0.16$	—	—
GALLEX			
(HAMPEL 99)[14]	—	$77.5 \pm 6.2^{+4.3}_{-4.7}$	—
GNO			
(ALTMANN 00)[15]	—	$65.8^{+10.2+3.4}_{-\ 9.6-3.6}$	—
SAGE			
(ABDURASHI...02)[16]	—	$70.8^{+5.3+3.7}_{-5.2-3.2}$	—
Kamiokande			
(FUKUDA 96)[17]	—	—	$2.80 \pm 0.19 \pm 0.33^{\dagger}$
Super-Kamiokande			
(FUKUDA 02)[18]	—	—	$2.35 \pm 0.03^{+0.07}_{-0.06}{}^{\dagger}$
SNO (pure D_2O)			
(AHMAD 02)[4]	—	—	$1.76^{+0.06}_{-0.05} \pm 0.09^{\ddagger}$
	—	—	$2.39^{+0.24}_{-0.23} \pm 0.12^{\dagger}$
	—	—	$5.09^{+0.44+0.46}_{-0.43-0.43}{}^{*}$
SNO (NaCl in D_2O)			
(AHMED 03)[8]	—	—	$1.59^{+0.08+0.06}_{-0.07-0.08}{}^{\ddagger}$
	—	—	$2.21^{+0.31}_{-0.26} \pm 0.10^{\dagger}$
	—	—	$5.21 \pm 0.27 \pm 0.38^{*}$
(BAHCALL 01)[9]	$7.6^{+1.3}_{-1.1}$	128^{+9}_{-7}	$5.05(1.00^{+0.20}_{-0.16})$
(TURCK-CHIEZE 01)[10]	7.44 ± 0.96	127.8 ± 8.6	4.95 ± 0.72

* Flux measured via the neutral-current reaction.

† Flux measured via νe elastic scattering.

‡ Flux measured via the charged-current reaction.

rates or flux from these experiments are listed in Table 2 and compared to the two recent solar-model predictions.

3.1. Radiochemical Experiments

Radiochemical experiments exploit electron neutrino absorption on nuclei followed by their decay through orbital electron capture. Produced Auger electrons are counted.

The Homestake chlorine experiment in USA uses the reaction

$$^{37}\mathrm{Cl} + \nu_e \rightarrow {}^{37}\mathrm{Ar} + e^- \ \text{(threshold 814 keV)}. \qquad (3)$$

Three gallium experiments (GALLEX and GNO at Gran Sasso in Italy and SAGE at Baksan in Russia) use the reaction

$$^{71}\mathrm{Ga} + \nu_e \rightarrow {}^{71}\mathrm{Ge} + e^- \ \text{(threshold 233 keV)}. \qquad (4)$$

The produced ^{37}Ar and ^{71}Ge atoms are both radioactive, with half lives ($\tau_{1/2}$) of 34.8 days and 11.43 days, respectively. After an exposure of the detector for two to three times $\tau_{1/2}$, the reaction products are chemically extracted and introduced into a low-background proportional counter, where they are counted for a sufficiently long period to determine the exponentially decaying signal and a constant background.

Solar-model calculations predict that the dominant contribution in the chlorine experiment comes from ^{8}B neutrinos, but ^{7}Be, *pep*, ^{13}N, and ^{15}O neutrinos also contribute. At present, the most abundant *pp* neutrinos can be detected only in gallium experiments. Even so, according to the solar-model calculations, almost half of the capture rate in the gallium experiments is due to other solar neutrinos.

The Homestake chlorine experiment was the first to attempt the observation of solar neutrinos. Initial results obtained in 1968 showed no events above background with upper limit for the solar-neutrino flux of 3 SNU [1]. After introduction

of an improved electronics system which discriminates signal from background by measuring the rise time of the pulses from proportional counters, a finite solar-neutrino flux has been observed since 1970. The solar-neutrino capture rate shown in Table 2 is a combined result of 108 runs between 1970 and 1994 [13]. It is only about 1/3 of the BP2000 prediction [9].

GALLEX presented the first evidence of *pp* solar-neutrino observation in 1992 [19]. Here also, the observed capture rate is significantly less than the SSM prediction. SAGE initially reported very low capture rate, $20^{+15}_{-20} \pm 32$ SNU, with a 90% confidence-level upper limit of 79 SNU [20]. Later, SAGE observed similar capture rate to that of GALLEX [21]. Both GALLEX and SAGE groups tested the overall detector response with intense man-made ^{51}Cr neutrino sources, and observed good agreement between the measured ^{71}Ge production rate and that predicted from the source activity, demonstrating the reliability of these experiments. The GALLEX Collaboration formally finished observations in early 1997. Since April, 1998, a newly defined collaboration, GNO (Gallium Neutrino Observatory) resumed the observations.

3.2 Kamiokande and Super-Kamiokande

Kamiokande and Super-Kamiokande in Japan are real-time experiments utilizing νe scattering

$$\nu_x + e^- \rightarrow \nu_x + e^- \tag{5}$$

in a large water-Cherenkov detector. It should be noted that the reaction Eq. (5) is sensitive to all active neutrinos, $x = e$, μ, and τ. However, the sensitivity to ν_μ and ν_τ is much smaller than the sensitivity to ν_e, $\sigma(\nu_{\mu,\tau}e) \approx 0.16\,\sigma(\nu_e e)$. The solar-neutrino flux measured via νe scattering is deduced assuming no neutrino oscillations.

These experiments take advantage of the directional correlation between the incoming neutrino and the recoil electron. This feature greatly helps the clear separation of the solar-neutrino signal from the background. Due to the high thresholds (7 MeV in Kamiokande and 5 MeV at present in Super-Kamiokande) the experiments observe pure ^{8}B solar neutrinos because *hep* neutrinos contribute negligibly according to the SSM.

The Kamiokande-II Collaboration started observing ^{8}B solar neutrinos at the beginning of 1987. Because of the strong directional correlation of νe scattering, this result gave the first direct evidence that the Sun emits neutrinos [22] (no directional information is available in radiochemical solar-neutrino experiments). The observed solar-neutrino flux was also significantly less than the SSM prediction. In addition, Kamiokande-II obtained the energy spectrum of recoil electrons and the fluxes separately measured in the daytime and nighttime. The Kamiokande-II experiment came to an end at the beginning of 1995.

Super-Kamiokande is a 50-kton second-generation solar-neutrino detector, which is characterized by a significantly larger counting rate than the first-generation experiments. This experiment started observation in April 1996. The solar-neutrino flux was measured as a function of zenith angle and recoil-electron energy [18]. The average solar-neutrino flux was smaller than, but consistent with, the Kamiokande-II result [17]. The observed day-night asymmetry was $A_{\rm DN} = \dfrac{\rm Day - Night}{0.5(\rm Day + Night)} = -0.021 \pm 0.020^{+0.013}_{-0.012}$. No indication of spectral distortion was observed.

In November 2001, Super-Kamiokande suffered from an accident in which substantial number of photomultiplier tubes were lost. The detector was rebuilt within a year with about half

of the original number of photomultiplier tubes. The experiment with the detector before the accident is now called Super-Kamiokande-I, and that after the accident is called Super-Kamiokande-II.

3.3 SNO

In 1999, a new real time solar-neutrino experiment, SNO, in Canada started observation. This experiment uses 1000 tons of ultra-pure heavy water (D_2O) contained in a spherical acrylic vessel, surrounded by an ultra-pure H_2O shield. SNO measures ^{8}B solar neutrinos via the reactions

$$\nu_e + d \rightarrow e^- + p + p \tag{6}$$

and

$$\nu_x + d \rightarrow \nu_x + p + n, \tag{7}$$

as well as νe scattering, Eq. (5). The CC reaction, Eq. (6), is sensitive only to electron neutrinos, while the NC reaction, Eq. (7), is sensitive to all active neutrinos.

The Q-value of the CC reaction is -1.4 MeV and the electron energy is strongly correlated with the neutrino energy. Thus, the CC reaction provides an accurate measure of the shape of the ^{8}B solar-neutrino spectrum. The contributions from the CC reaction and νe scattering can be distinguished by using different cos $\theta_\odot$ distributions where $\theta_\odot$ is the angle of the electron momentum with respect to the direction from the Sun to the Earth. While the νe scattering events have a strong forward peak, CC events have an approximate angular distribution of $1 - 1/3\ \cos\theta_\odot$.

The threshold of the NC reaction is 2.2 MeV. In the pure D_2O, the signal of the NC reaction is neutron capture in deuterium, producing a 6.25-MeV γ-ray. In this case, the capture efficiency is low and the deposited energy is close to

the detection threshold of 5 MeV. In order to enhance both the capture efficiency and the total γ-ray energy (8.6 MeV), 2 tons of NaCl were added to the heavy water in the second phase of the experiment. In addition, installation of discrete ^{3}He neutron counters is planned for the NC measurement in the third phase.

In 2001, SNO published the initial results on the measurement of the ^{8}B solar-neutrino flux via CC reaction [2]. The electron energy spectrum and the $\cos\theta_\odot$ distribution were also measured. The spectral shape of the electron energy was consistent with the expectations for an undistorted ^{8}B solar-neutrino spectrum.

SNO also measured the ^{8}B solar-neutrino flux via νe scattering. Though the latter result had poor statistics, it was consistent with the high-statistics Super-Kamiokande result. Thus, the SNO group compared their CC result with Super-Kamiokande's νe scattering result, and obtained evidence of an active non-ν_e component in the solar-neutrino flux, as further described in Sec. 3.5.

Later, in April, 2002, SNO reported the first result on the ^{8}B solar-neutrino flux measurement via NC reaction [4]. The total flux measured via NC reaction was consistent with the solar-model predictions (see Table 2). Also, the SNO's CC and νe scattering results were updated [4]. These results were consistent with the earlier results [2].

Further, the day and night energy spectra were measured and the day-night asymmetry of the ν_e flux measured with CC events was presented [23]. Assuming an undistorted ^{8}B spectrum, the asymmetry was $A_{\rm DN} = \dfrac{\rm Day - Night}{0.5(\rm Day + Night)} =$

$-0.140 \pm 0.063^{+0.015}_{-0.014}$. With an additional constraint of no asymmetry for the total flux of active neutrinos, the asymmetry was found to be $-0.070 \pm 0.049^{+0.013}_{-0.012}$.

The SNO Collaboration made a global analysis (see Sect. 3.6) of the SNO's day and night energy spectra together with the data from other solar-neutrino experiments. The results strongly favored the LMA solution, with the LOW solution allowed at 99.5% confidence level [23]. (In most of the similar global analyses, the VAC solution was also allowed at $99.9 \sim 99.73\%$ confidence level, see Sect. 3.6.) For the LMA solution (and also for the LOW solution), the maximal mixing was excluded at $> 3\sigma$.

Recently, in September, 2003, SNO has released the results of solar-neutrino flux measurements with dissolved NaCl in the heavy water. The results from the "salt phase" are described in Sect. 5.

3.4 Comparison of Experimental Results with Solar-Model Predictions

It is clear from Table 2 that the results from all the solar-neutrino experiments, except the SNO's NC result, indicate significantly less flux than expected from the BP2000 SSM [9] and the Turck-Chieze *et al.* solar model [10].

There has been a consensus that a consistent explanation of all the results of solar-neutrino observations is unlikely within the framework of astrophysics using the solar-neutrino spectra given by the standard electroweak model. Many authors made solar model-independent analyses constrained by the observed solar luminosity [24–28], where they attempted to fit the measured solar-neutrino capture rates and ^{8}B flux with normalization-free, undistorted energy spectra. All these attempts only obtained solutions with very low probabilities.

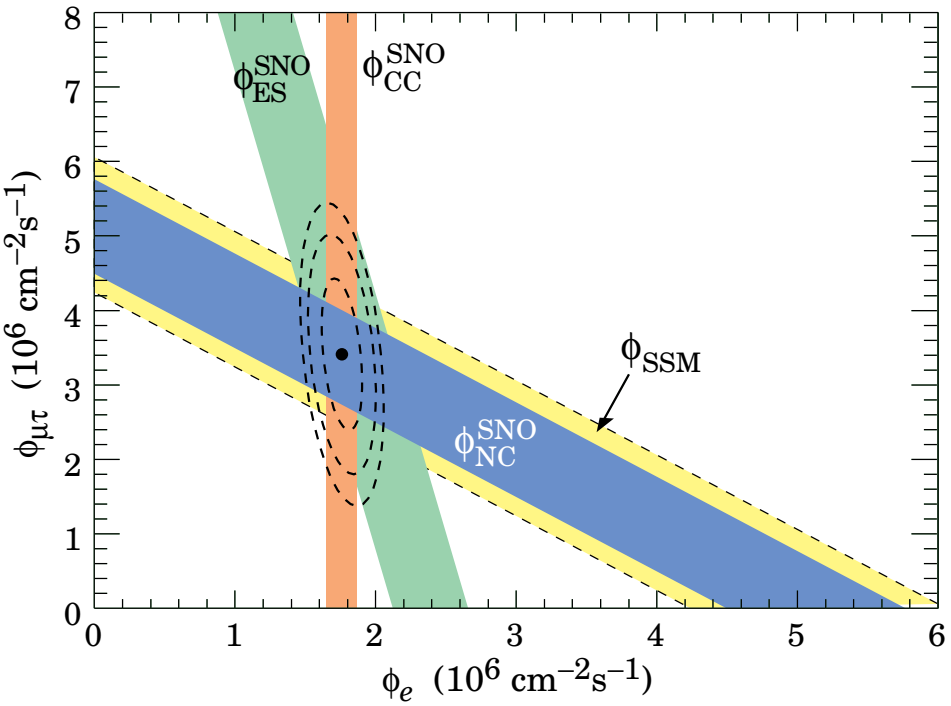

Figure 2: Fluxes of ^{8}B solar neutrinos, $\phi(\nu_e)$, and $\phi(\nu_{\mu \text{ or } \tau})$, deduced from the SNO's charged-current (CC), ν_e elastic scattering (ES), and neutral-current (NC) results for pure D_2O. The standard solar model prediction [9] is also shown. The bands represent the 1σ error. The contours show the 68%, 95%, and 99% joint probability for $\phi(\nu_e)$ and $\phi(\nu_{\mu \text{ or } \tau})$. This figure is courtesy of K.T. Lesko (LBNL). See full-color version on color pages at end of book.

The data therefore suggest that the solution to the solar-neutrino problem requires nontrivial neutrino properties.

3.5 Evidence for Solar Neutrino Oscillations

Denoting the ^{8}B solar-neutrino flux obtained by the SNO's CC measurement as $\phi^{CC}_{SNO}(\nu_e)$ and that obtained by the Super-Kamiokande νe scattering as $\phi^{ES}_{SK}(\nu_x)$, $\phi^{CC}_{SNO}(\nu_e) = \phi^{ES}_{SK}(\nu_x)$ is

expected for the standard neutrino physics. However, SNO's initial data [2] indicated

$$\phi^{\rm ES}_{\rm SK}(\nu_x) - \phi^{\rm CC}_{\rm SNO}(\nu_e) = (0.57 \pm 0.17) \times 10^6 \ \ {\rm cm}^{-2}{\rm s}^{-1}. \qquad (8)$$

The significance of the difference was $> 3\sigma$, implying direct evidence for the existence of a non-ν_e active neutrino flavor component in the solar-neutrino flux. A natural and most probable explanation of neutrino flavor conversion is neutrino oscillation. Note that both the SNO [2] and Super-Kamiokande [3] flux results were obtained by assuming the standard ^{8}B neutrino spectrum shape. This assumption was justified by the measured energy spectra in both of the experiments.

The SNO's results for pure D_2O, reported in 2002 [4], provided stronger evidence for neutrino oscillation than Eq. (8). The fluxes measured with CC, ES and NC events were

$$\phi^{\rm CC}_{\rm SNO}(\nu_e) = (1.76^{+0.06}_{-0.05} \pm 0.09) \times 10^6 {\rm cm}^{-2}{\rm s}^{-1} \ , \qquad (9)$$

$$\phi^{\rm ES}_{\rm SNO}(\nu_x) = (2.39^{+0.24}_{-0.23} \pm 0.12) \times 10^6 {\rm cm}^{-2}{\rm s}^{-1} \ , \qquad (10)$$

$$\phi^{\rm NC}_{\rm SNO}(\nu_x) = (5.09^{+0.44+0.46}_{-0.43-0.43}) \times 10^6 {\rm cm}^{-2}{\rm s}^{-1} \ . \qquad (11)$$

Eq. (11) is a mixing-independent result and therefore tests solar models. It shows very good agreement with the ^{8}B solar-neutrino flux predicted by the BP2000 SSM [9] and that predicted by Turck-Chieze *et al.* model [10]. The fluxes $\phi(\nu_e)$ and $\phi(\nu_{\mu \text{ or } \tau})$ deduced from these results were remarkably consistent as can be seen in Fig. 2. The resultant flux of non-ν_e active neutrinos, $\phi(\nu_{\mu \text{ or } \tau})$, was

$$\phi(\nu_{\mu \text{ or } \tau}) = \left(3.41^{+0.66}_{-0.64}\right) \times 10^6 {\rm cm}^{-2}{\rm s}^{-1} \qquad (12)$$

where the statistical and systematic errors were added in quadrature. This $\phi(\nu_{\mu \text{ or } \tau})$ was 5.3 σ above 0.

3.6. Pre-KamLAND Global Analyses of the Solar Neutrino Data

A global analysis of the solar-neutrino data essentially uses all the independent solar-neutrino data that are available when the analysis is made to determine the globally allowed regions in terms of two neutrino oscillations either in vacuum or in matter. A number of pre-SNO global analyses of the solar-neutrino data yielded various solutions. (For example, see Ref. [29].) With the SNO's CC and NC measurements, various global analyses [30–36] showed that LMA was the most favored solution, but either or both of the two other solutions, LOW (low probability or low mass) and VAC (vacuum), were marginally allowed at $99.9 \sim 99.73\%$ confidence level. These global analyses mostly differ in the statistical treatment of the data.

Typical parameter values [34] corresponding to these solutions are

- LMA: $\Delta m^2 = 5.5 \times 10^{-5}$ eV^2, $\tan^2\theta = 0.42$
- LOW: $\Delta m^2 = 7.3 \times 10^{-8}$ eV^2, $\tan^2\theta = 0.67$
- VAC: $\Delta m^2 = 6.5 \times 10^{-10}$ eV^2, $\tan^2\theta = 1.33$.

It should be noted that all these solutions have large mixing angles. SMA (small mixing angle) solution (typical parameter values [34] are $\Delta m^2 = 5.2 \times 10^{-6}$ eV^2 and $\tan^2\theta = 1.1 \times 10^{-3}$) was once favored, but after SNO it was excluded at $> 3\sigma$ [30–36].

4. KamLAND and Combined Oscillation Analysis

KamLAND is a 1-kton ultra-pure liquid scintillator detector located at the old Kamiokande's site in Japan. Although the ultimate goal of KamLAND is observation of ^{7}Be solar neutrinos with much lower energy threshold, the initial phase of the experiment is a long baseline (flux-weighted average distance of ~ 180 km) neutrino oscillation experiment using $\bar{\nu}_e$'s emitted

from power reactors. The reaction $\bar{\nu}_e + p \to e^+ + n$ is used to detect reactor $\bar{\nu}_e$'s and delayed coincidence with 2.2 MeV γ-ray from neutron capture on a proton is used to reduce the backgrounds.

With the reactor $\bar{\nu}_e$'s energy spectrum (< 8 MeV) and an analysis threshold of 2.6 MeV, this experiment has a sensitive Δm^2 range down to $\sim 10^{-5}$ eV^2. Therefore, if the LMA solution is the real solution of the solar neutrino problem, KamLAND should observe reactor $\bar{\nu}_e$ disappearance, assuming CPT invariance.

The first KamLAND results [7] with live time of 145 days were reported in December 2002. The ratio of observed to expected (assuming no neutrino oscillation) number of events was

$$\frac{N_{\rm obs} - N_{\rm BG}}{N_{\rm NoOsc}} = 0.611 \pm 0.085 \pm 0.041. \qquad (13)$$

with obvious notation. This result shows clear evidence of event deficit expected from neutrino oscillation. The 95% confidence level allowed regions shown in Fig. 3 are obtained from the oscillation analysis with the observed event rates and positron spectrum shape. In this figure, the allowed region for the LMA solution from a global analysis [34] of the solar-neutrino data is also shown. There are two bands of regions allowed by both solar and KamLAND data. The LOW and VAC solutions are excluded by the KamLAND results.

A combined global solar and KamLAND analysis shows that the LMA is a unique solution to the solar neutrino problem with $> 5\sigma$ confidence level [37]. The 99% confidence level allowed region from combined analyses [37–45] splits into two subregions. At $> 3\sigma$ these subregions become connected.

5. SNO Salt Phase Results

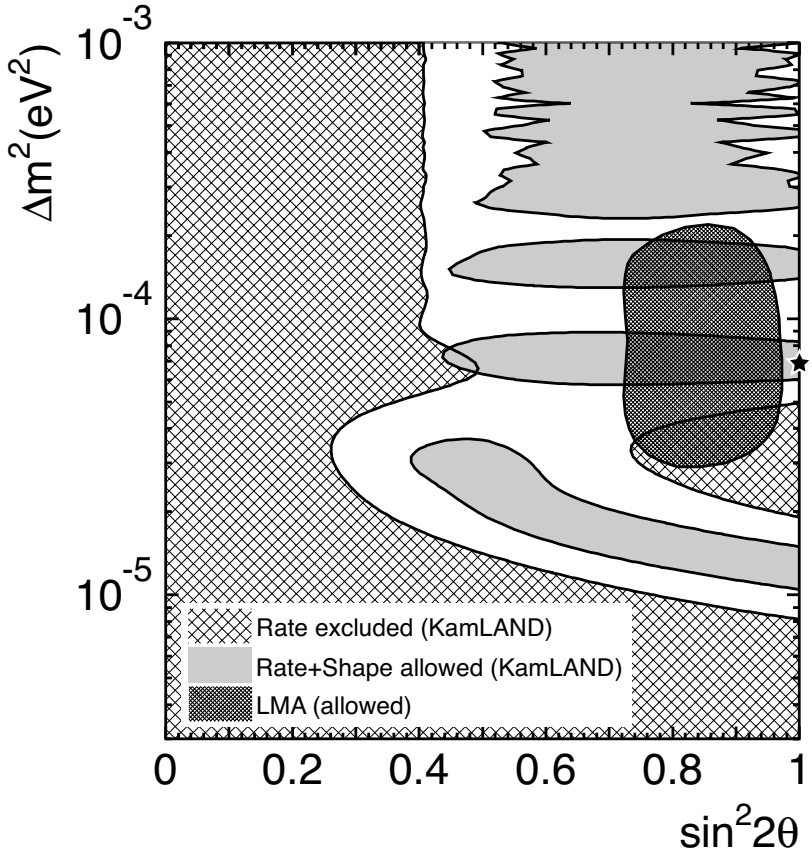

Figure 3: Excluded regions of neutrino oscillation parameters for the rate analysis and allowed regions for the combined rate and shape analysis from KamLAND at 95% confidence level. The 95% confidence-level allowed region of the LMA solution taken from a global analysis by Fogli *et al.* [34] is also shown. The star shows the best fit to the KamLAND data in the physical region: $\sin^2 2\theta = 1.0$ and $\Delta m^2 = 6.9 \times 10^{-5}$ eV^2. All regions look identical under $\theta \leftrightarrow (\pi/2 - \theta)$ except for the LMA region from solar-neutrino experiments. This figure is courtesy of K. Inoue (Tohoku University).

The SNO Collaboration recently reported the total ^{8}B solar-neutrino flux measured via NC reaction with NaCl dissolved in the detector heavy water [8]. The accuracy in the flux measurement has improved compared to the previous measurements thanks to the enhanced sensitivity to NC reactions (see Table 2). These results further constrain the allowed region of the LMA solution (see Fig. 4). A global analysis of the solar-neutrino data combined with the KamLAND data has shrunk the allowed region to the lower Δm^2 band at 99% confidence level with the best fit point at $\Delta m^2 = 7.1^{+1.2}_{-0.6} \times 10^{-5}$ eV^2 and $\theta = 32.5^{+2.4}_{-2.3}$ degrees [8]. The maximal mixing is now excluded at $> 5\sigma$ confidence level [8]. Other combined analyses give consistent results [46–51].

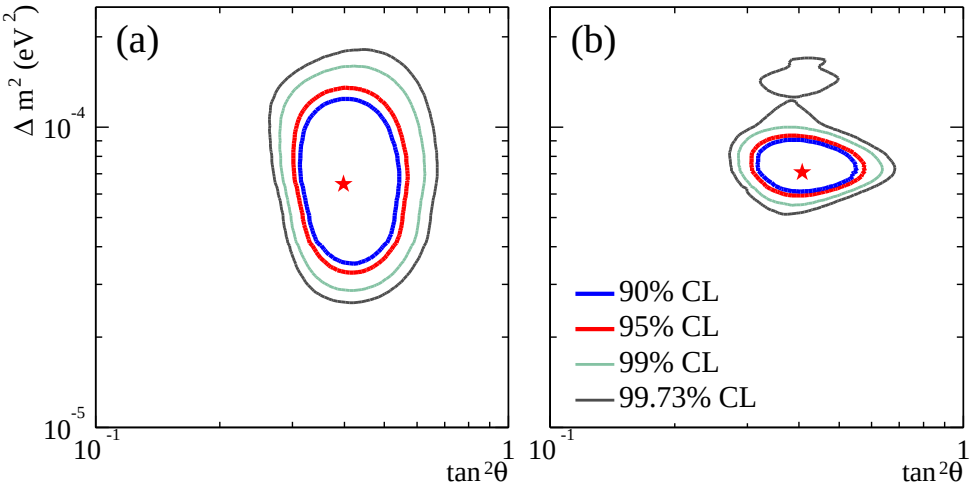

Figure 4: Global neutrino oscillation contours given by the SNO Collaboration assuming that the ^{8}B neutrino flux is free and the *hep* neutrino flux is fixed. (a) Solar global analysis. (b) Solar global + KamLAND. For details, see Ref. [8]. See full-color version on color pages at end of book.

6. Future Prospects

Now that the solar-neutrino problem has been essentially solved, what are the future prospects of the solar-neutrino experiments?

From the particle-physics point of view, precise determination of the oscillation parameters and search for non-standard physics such as a small admixture of a sterile component in the solar-neutrino flux will be still of interest. To determine Δm^2 more precisely, further KamLAND exposure to the reactor neutrinos will be most powerful [46,53]. More precise NC measurements by SNO will contribute in reducing the uncertainty of the mixing angle [51,53]. Measurements of the pp flux to an accuracy comparable to the quoted accuracy ($\pm 1\%$) of the SSM calculation will significantly improve the precision of the mixing angle [46,53].

An important task of the future solar neutrino experiments is further tests of the SSM by measuring monochromatic ^{7}Be neutrinos and fundamental *pp* neutrinos. The ^{7}Be neutrino flux will be measured by a new experiment, Borexino, at Gran Sasso via νe scattering in 300 tons of ultra-pure liquid scintillator with a detection threshold as low as 250 keV. KamLAND will also observe ^{7}Be neutrinos if the detection threshold can be lowered to a level similar to that of Borexino.

For the detection of *pp* neutrinos, various ideas for the detection scheme have been presented. However, no experiments have been approved yet, and extensive R&D efforts are still needed for any of these ideas to prove its feasibility.

References

1. D. Davis, Jr., D.S. Harmer, and K.C. Hoffman, Phys. Rev. Lett. **20**, 1205 (1968).
2. Q.R. Ahmad *et al.*, Phys. Rev. Lett. **87**, 071301 (2001).

3. Y. Fukuda *et al.*, Phys. Rev. Lett. **86**, 5651 (2001).
4. Q.R. Ahmad *et al.*, Phys. Rev. Lett. **89**, 011301 (2002).
5. L. Wolfenstein, Phys. Rev. **D17**, 2369 (1978).
6. S.P. Mikheyev and A. Yu. Smirnov, Sov. J. Nucl. Phys. **42**, 913 (1985).
7. K. Eguchi *et al.*, Phys. Rev. Lett. **90**, 021802 (2003).
8. S.N. Ahmed *et al.*, `nucl-ex/03090034`.
9. J.N. Bahcall, M.H. Pinsonneault, and S. Basu, Astrophys. J. **555**, 990 (2001).
10. S. Turck-Chieze *et al.*, Astrophys. J. **555**, L69 (2001).
11. A.R. Junghans *et al.*, Phys. Rev. Lett. **88**, 041101 (2002).
12. J.N. Bahcall, M.C. Gonzalez-Garcia, and C. Peña-Garay, JHEP **04**, 007 (2002).
13. B.T. Cleveland *et al.*, Ap. J. **496**, 505 (1998).
14. W. Hampel *et al.*, Phys. Lett. **B447**, 127 (1999).
15. M. Altmann *et al.*, Phys. Lett. **B490**, 16 (2000).
16. J.N. Abdurashitov *et al.*, Sov. Phys. JETP **95**, 181 (2002).
17. Y. Fukuda *et al.*, Phys. Rev. Lett. **77**, 1683 (1996).
18. Y. Fukuda *et al.*, Phys. Lett. **B539**, 179 (2002).
19. P. Anselmann *et al.*, Phys. Lett. **B285**, 376 (1994).
20. A.I. Abazov *et al.*, Phys. Rev. Lett. **67**, 3332 (1991).
21. J.N. Abdurashitov *et al.*, Phys. Lett. **B328**, 234 (1994).
22. K.S. Hirata *et al.*, Phys. Rev. Lett. **63**, 16 (1989).
23. Q.R. Ahmad *et al.*, Phys. Rev. Lett. **89**, 011302 (2002).
24. N. Hata, S. Bludman, and P. Langacker, Phys. Rev. **D49**, 3622 (1994).
25. N. Hata and P. Langacker, Phys. Rev. **D52**, 420 (1995).
26. N. Hata and P. Langacker, Phys. Rev. **D56**, 6107 (1997).
27. S. Parke, Phys. Rev. Lett. **74**, 839 (1995).
28. K.M. Heeger and R.G.H. Robertson, Phys. Rev. Lett. **77**, 3720 (1996).
29. J.N. Bahcall, P.I. Krastev, and A.Yu. Smirnov, JHEP, 05, 015 (2001).

30. V. Barger *et al.*, Phys. Lett. **B537**, 179 (2002).
31. A. Bandyopadhyay *et al.*, Phys. Lett. **B540**, 14 (2002).
32. J.N. Bahcall, C.M. Gonzalez-Garcia, and C. Peña-Garay, JHEP 07, 054 (2002).
33. A. Strumia *et al.*, Phys. Lett. **B541**, 327 (2002).
34. G.L. Fogli *et al.*, Phys. Rev. **D66**, 053010 (2002).
35. P.C. de Holanda and A. Yu Smirnov, Phys. Rev. **D66**, 113005 (2002).
36. M. Maltoni *et al.*, Phys. Rev. **D67**, 013011 (2003).
37. J.N. Bahcall, M.C. Gonzalez-Garcia, and C. Peña-Garay, JHEP 02, 009 (2003).
38. G.L. Fogli *et al.*, Phys. Rev. **D67**, 073002 (2003).
39. V. Barger and D. Marfatia Phys. Lett. **B555**, 144 (2003).
40. M. Maltoni *et al.*, Phys. Rev. **D67**, 093003 (2003).
41. A. Bandyopadhyay *et al.*, Phys. Lett. **B559**, 121 (2003).
42. P.C. de Holanda and A. Yu Smirnov, JCAP 02, 001 (2003).
43. A.B. Balantekin and H. Yüksel, J. Phys. **G29**, 665 (2003).
44. H. Nunokawa, W.J.C. Tevas, and R. Zukanovich Funchal, Phys. Lett. **B562**, 28 (2003).
45. P. Aliani *et al.*, `hep-ph/0212212`.
46. J.N. Bahcall and C. Peña-Garay, `hep-ph/0305159`.
47. A.B. Balantekin and H. Yüksel, `hep-ph/0309079`.
48. G.L. Fogli *et al.*, `hep-ph/0309100`.
49. M. Maltoni *et al.*, `hep-ph/0309130`.
50. P. Aliani *et al.*, `hep-ph/0309156`.
51. A. Bandyopadhyay *et al.*, `hep-ph/0309174`.
52. P.C. de Holanda and A. Yu Smirnov, `hep-ph/0309299`.
53. A. Bandyopadhyay, S. Choubey, and S. Goswami, Phys. Rev. **D67**, 113011 (2003).

ν_e Capture Rates from Radiochemical Experiments

1 SNU (Solar Neutrino Unit) = 10^{-36} captures per atom per second.

VALUE (SNU)	DOCUMENT ID		TECN	COMMENT
$70.8 \begin{smallmatrix}+5.3\\-5.2\end{smallmatrix} \begin{smallmatrix}+3.7\\-3.2\end{smallmatrix}$	[166] ABDURASHI...	02	SAGE	$^{71}Ga \rightarrow {}^{71}Ge$
$65.8 \begin{smallmatrix}+10.2\\-9.6\end{smallmatrix} \begin{smallmatrix}+3.4\\-3.6\end{smallmatrix}$	[167] ALTMANN	00	GNO	$^{71}Ga \rightarrow {}^{71}Ge$
$74.1 \begin{smallmatrix}+6.7\\-6.8\end{smallmatrix}$	[168] ALTMANN	00	GNO	GNO + GALX combined
$77.5 \pm 6.2 \begin{smallmatrix}+4.3\\-4.7\end{smallmatrix}$	[169] HAMPEL	99	GALX	$^{71}Ga \rightarrow {}^{71}Ge$
$2.56 \pm 0.16 \pm 0.16$	[170] CLEVELAND	98	HOME	$^{37}Cl \rightarrow {}^{37}Ar$

[166] ABDURASHITOV 02 report a combined analysis of 92 runs of the SAGE solar-neutrino experiment during the period January 1990 through December 2001, and updates the ABDURASHITOV 99B result. A total of 406.4 ^{71}Ge events were observed. No evidence was found for temporal variations of the neutrino capture rate over the entire observation period.

[167] ALTMANN 00 report the first result from the GNO solar-neutrino experiment (GNO I), which is the successor project of GALLEX. Experimental technique of GNO is essentially the same as that of GALLEX. The run data cover the period 20 May 1998 through 12 January 2000.

[168] Combined result of GALLEX I+II+III+IV (HAMPEL 99) and GNO I. The indicated errors include systematic errors.

[169] HAMPEL 99 report the combined result for GALLEX I+II+III+IV (65 runs in total), which update the HAMPEL 96 result. The GALLEX IV result (12 runs) is 118.4 $\pm$ 17.8 $\pm$ 6.6 SNU. (HAMPEL 99 discuss the consistency of partial results with the mean.) The GALLEX experimental program has been completed with these runs. The total run data cover the period 14 May 1991 through 23 January 1997. A total of 300 ^{71}Ge events were observed.

[170] CLEVELAND 98 is a detailed report of the ^{37}Cl experiment at the Homestake Mine. The average solar neutrino-induced ^{37}Ar production rate from 108 runs between 1970 and 1994 updates the DAVIS 89 result.

ϕ_{ES} (^{8}B)

^{8}B solar-neutrino flux measured via νe elastic scattering. This process is sensitive to all active neutrino flavors, but with reduced sensitivity to ν_μ, ν_τ due to the cross-section difference, $\sigma(\nu_{\mu,\tau} e) \sim 0.16\sigma(\nu_e e)$. If the ^{8}B solar-neutrino flux involves nonelectron flavor active neutrinos, their contribution to the flux is $\sim$ 0.16 times of ν_e.

VALUE (10^6 cm^{-2}s^{-1})	DOCUMENT ID		TECN	COMMENT
$2.35 \begin{smallmatrix}+0.07\\-0.06\end{smallmatrix}$ OUR AVERAGE				
$2.39 \begin{smallmatrix}+0.24\\-0.23\end{smallmatrix} \pm 0.12$	[171] AHMAD	02	SNO	average flux
$2.35 \pm 0.03 \begin{smallmatrix}+0.07\\-0.06\end{smallmatrix}$	[172] FUKUDA	02	SKAM	average flux
• • • We do not use the following data for averages, fits, limits, etc. • • •				
$2.39 \pm 0.34 \begin{smallmatrix}+0.16\\-0.14\end{smallmatrix}$	[173] AHMAD	01	SNO	average flux
$2.80 \pm 0.19 \pm 0.33$	[174] FUKUDA	96	KAMI	average flux
2.70 ± 0.27	[174] FUKUDA	96	KAMI	day flux
$2.87 \begin{smallmatrix}+0.27\\-0.26\end{smallmatrix}$	[174] FUKUDA	96	KAMI	night flux

[171] AHMAD 02 reports the ^{8}B solar-neutrino flux measured via νe elastic scattering above the kinetic energy threshold of 5 MeV. The data correspond to 306.4 live days with SNO between November 2, 1999 and May 28, 2001, and updates AHMAD 01 results.

[172] FUKUDA 02 results are for 1496 live days with Super-Kamiokande between May 31, 1996 and July 15, 2002, and replace FUKUDA 01 results. The analysis threshold is 5 MeV except for the first 280 live days (6.5 MeV).

[173] AHMAD 01 reports the ^{8}B solar-neutrino flux measured via νe elastic scattering above the kinetic energy threshold of 6.75 MeV. The data correspond to 241 live days with SNO between November 2, 1999 and January 15, 2001.

[174] FUKUDA 96 results are for a total of 2079 live days with Kamiokande II and III from January 1987 through February 1995, covering the entire solar cycle 22, with threshold $E_e > 9.3$ MeV (first 449 days), > 7.5 MeV (middle 794 days), and > 7.0 MeV (last 836 days). These results update the HIRATA 90 result for the average ^{8}B solar-neutrino flux and HIRATA 91 result for the day-night variation in the ^{8}B solar-neutrino flux. The total data sample was also analyzed for short-term variations: within experimental errors, no strong correlation of the solar-neutrino flux with the sunspot numbers was found.

ϕ_{CC} (^{8}B)

^{8}B solar-neutrino flux measured with charged-current reaction which is sensitive exclusively to ν_e.

VALUE (10^6 cm^{-2}s^{-1})	DOCUMENT ID		TECN	COMMENT
$1.76^{+0.06}_{-0.05} \pm 0.09$	[175] AHMAD	02	SNO	average flux
• • • We do not use the following data for averages, fits, limits, etc. • • •				
$1.75 \pm 0.07^{+0.12}_{-0.11} \pm 0.05$	[176] AHMAD	01	SNO	average flux

[175] AHMAD 02 reports the SNO result of the ^{8}B solar-neutrino flux measured with charged-current reaction on deuterium, $\nu_e d \rightarrow pp e^-$, above the kinetic energy threshold of 5 MeV. The data correspond to 306.4 live days with SNO between November 2, 1999 and May 28, 2001, and updates AHMAD 01 results.

[176] AHMAD 01 reports the first SNO result of the ^{8}B solar-neutrino flux measured with the charged-current reaction on deuterium, $\nu_e d \rightarrow pp e^-$, above the kinetic energy threshold of 6.75 MeV. The data correspond to 241 live days with SNO between November 2, 1999 and January 15, 2001.

ϕ_{NC} (^{8}B)

^{8}B solar neutrino flux measured with neutral-current reaction, which is equally sensitive to ν_e, ν_μ, and ν_τ.

VALUE (10^6 cm^{-2}s^{-1})	DOCUMENT ID		TECN	COMMENT
$5.09^{+0.44+0.46}_{-0.43-0.43}$	[177] AHMAD	02	SNO	average flux

[177] AHMAD 02 reports the first SNO result of the ^{8}B solar-neutrino flux measured with the neutral-current reaction on deuterium, $\nu_\ell d \rightarrow np\nu_\ell$, above the neutral-current reaction threshold of 2.2 MeV. The data correspond to 306.4 live days with SNO between November 2, 1999 and May 28, 2001.

$\phi_{\nu_\mu+\nu_\tau}$ (^{8}B)

Nonelectron-flavor active neutrino component (ν_μ and ν_τ) in the ^{8}B solar-neutrino flux.

VALUE (10^6 cm^{-2}s^{-1})	DOCUMENT ID		TECN	COMMENT
$3.41 \pm 0.45 ^{+0.48}_{-0.45}$	[178] AHMAD	02	SNO	Derived from SNO ϕ_{CC}, ϕ_{ES}, and ϕ_{NC}
• • • We do not use the following data for averages, fits, limits, etc. • • •				
3.69 ± 1.13	[179] AHMAD	01		Derived from SNO+SuperKam, water Cherenkov

[178] AHMAD 02 deduced the nonelectron-flavor active neutrino component (ν_μ and ν_τ) in the ^{8}B solar-neutrino flux, by combining the charged-current result, the νe elastic-scattering result and the neutral-current result.

[179] AHMAD 01 deduced the nonelectron-flavor active neutrino component (ν_μ and ν_τ) in the ^{8}B solar-neutrino flux, by combining the SNO charged-current result (AHMAD 01) and the Super-Kamiokande νe elastic-scattering result (FUKUDA 01).

Total Flux of Active ^{8}B Solar Neutrinos

Total flux of active neutrinos (ν_e, ν_μ, and ν_τ).

VALUE (10^6 cm^{-2}s^{-1})	DOCUMENT ID		TECN	COMMENT
$5.09 ^{+0.44}_{-0.43} ^{+0.46}_{-0.43}$	[180] AHMAD	02	SNO	Direct measurement from ϕ_{NC}
5.44 ± 0.99	[181] AHMAD	01		Derived from SNO+SuperKam, water Cherenkov

[180] AHMAD 02 determined the total flux of active ^{8}B solar neutrinos by directly measuring the neutral-current reaction, $\nu_\ell d \rightarrow n p \nu_\ell$, which is equally sensitive to ν_e, ν_μ, and ν_τ.

[181] AHMAD 01 deduced the total flux of active ^{8}B solar neutrinos by combining the SNO charged-current result (AHMAD 01) and the Super-Kamiokande νe elastic-scattering result (FUKUDA 01).

Day-Night Asymmetry (^{8}B)

$A = (\phi_{\text{night}} - \phi_{\text{day}}) / \phi_{\text{average}}$

VALUE	DOCUMENT ID		TECN	COMMENT
$0.14 \pm 0.063 ^{+0.015}_{-0.014}$	[182] AHMAD	02B	SNO	Derived from SNO ϕ_{CC}
$0.07 \pm 0.049 ^{+0.013}_{-0.012}$	[183] AHMAD	02B	SNO	Constraint of no ϕ_{NC} asymmetry
$0.021 \pm 0.020 ^{+0.013}_{-0.012}$	[184] FUKUDA	02	SKAM	Based on ϕ_{ES}

[182] AHMAD 02B results are based on the charged-current interactions recorded between November 2, 1999 and May 28, 2001, with the day and night live times of 128.5 and 177.9 days, respectively.

[183] AHMAD 02B results are derived from the charged-current interactions, neutral-current interactions, and νe elastic scattering, with the total flux of active neutrinos constrained to have no asymmetry. The data were recorded between November 2, 1999 and May 28, 2001, with the day and night live times of 128.5 and 177.9 days, respectively.

[184] FUKUDA 02 results are for 1496 live days with Super-Kamiokande between May 31, 1996 and July 15, 2002, and replace FUKUDA 01 results. The analysis threshold is 5 MeV except for the first 280 live days (6.5 MeV).

ϕ_{ES} (hep)

hep solar-neutrino flux measured via νe elastic scattering. This process is sensitive to all active neutrino flavors, but with reduced sensitivity to ν_μ, ν_τ due to the cross-section difference, $\sigma(\nu_{\mu,\tau} e) \sim 0.16\sigma(\nu_e e)$. If the hep solar-neutrino flux involves nonelectron flavor active neutrinos, their contribution to the flux is ~ 0.16 times of ν_e.

VALUE (10^3 cm^{-2}s^{-1})	*CL%*	*DOCUMENT ID*		*TECN*
<40	90	[185] FUKUDA	01	SKAM

[185] FUKUDA 01 result is obtained from the recoil electron energy window of 18–21 MeV, and the obtained 90% confidence level upper limit is 4.3 times the BP2000 Standard-Solar-Model prediction.

REFERENCES FOR Neutrino Mixing

AHN	03	PRL 90 041801	M.H. Ahn *et al.*	(K2K Collab.)
AMBROSIO	03	PL B566 35	M. Ambrosio *et al.*	(MACRO Collab.)
APOLLONIO	03	EPJ C27 331	M. Apollonio *et al.*	(CHOOZ Collab.)
ASTIER	03	PL B570 19	P. Astier *et al.*	(NOMAD Collab.)
EGUCHI	03	PRL 90 021802	K. Eguchi *et al.*	(KamLAND Collab.)
ABDURASHI...	02	JETP 95 181	J.N. Abdurashitov *et al.*	(SAGE Collab.)
		Translated from ZETF 122 211.		
AHMAD	02	PRL 89 011301	Q.R. Ahmad *et al.*	(SNO Collab.)
AHMAD	02B	PRL 89 011302	Q.R. Ahmad *et al.*	(SNO Collab.)
ARMBRUSTER	02	PR D65 112001	B. Armbruster *et al.*	(KARMEN 2 Collab.)
AVVAKUNOV	02	PRL 89 011804	S. Avvakumov *et al.*	(NuTeV Collab.)
FUKUDA	02	PL B539 179	S. Fukuda *et al.*	(Super-Kamiokande Collab.)
AGUILAR	01	PR D64 112007	A. Aguilar *et al.*	(LSND Collab.)
AHMAD	01	PRL 87 071301	Q.R. Ahmad *et al.*	(SNO Collab.)
AMBROSIO	01	PL B517 59	M. Ambrosio *et al.*	(MACRO Collab.)
ASTIER	01B	NP B611 3	P. Astier *et al.*	(NOMAD Collab.)
BOEHM	01	PR D64 112001	F. Boehm *et al.*	
ESKUT	01	PL B497 8	E. Eskut *et al.*	(CHORUS Collab.)
FUKUDA	01	PRL 86 5651	S. Fukuda *et al.*	(Super-Kamiokande Collab.)
ALTMANN	00	PL B490 16	M. Altmann *et al.*	(GNO Collab.)
AMBROSIO	00	PL B478 5	M. Ambrosio *et al.*	(MACRO Collab.)
BOEHM	00	PRL 84 3764	F. Boehm *et al.*	
BOEHM	00C	PR D62 072002	F. Boehm *et al.*	
FUKUDA	00	PRL 85 3999	S. Fukuda *et al.*	(Super-Kamiokande Collab.)
ABDURASHI...	99B	PR C60 055801	J.N. Abdurashitov *et al.*	(SAGE Collab.)
ALLISON	99	PL B449 137	W.W.M. Allison *et al.*	(Soudan 2 Collab.)
APOLLONIO	99	PL B466 415	M. Apollonio *et al.*	(CHOOZ Collab.)
Also	00	PL B472 434 erratum	M. Apollonio *et al.*	(CHOOZ Collab.)
FUKUDA	99C	PRL 82 2644	Y. Fukuda *et al.*	(Super-Kamiokande Collab.)
FUKUDA	99D	PL B467 185	Y. Fukuda *et al.*	(Super-Kamiokande Collab.)
HAMPEL	99	PL B447 127	W. Hampel *et al.*	(GALLEX Collab.)
JUNK	99	NIM A434 435	T. Junk	
NAPLES	99	PR D59 031101	D. Naples *et al.*	(CCFR Collab.)
ALTEGOER	98B	PL B431 219	S. Altegoer *et al.*	(NOMAD Collab.)
AMBROSIO	98	PL B434 451	M. Ambrosio *et al.*	(MACRO Collab.)
APOLLONIO	98	PL B420 397	M. Apollonio *et al.*	(CHOOZ Collab.)
ARMBRUSTER	98	PR C57 3414	B. Armbruster *et al.*	(KARMEN Collab.)
ATHANASSO...	98	PRL 81 1774	C. Athanassopoulos *et al.*	(LSND Collab.)
ATHANASSO...	98B	PR C58 2489	C. Athanassopoulos *et al.*	(LSND Collab.)
CLEVELAND	98	APJ 496 505	B.T. Cleveland *et al.*	(Homestake Collab.)
ESKUT	98	PL B424 202	E. Eskut *et al.*	(CHORUS Collab.)
ESKUT	98B	PL B434 205	E. Eskut *et al.*	(CHORUS Collab.)
FELDMAN	98	PR D57 3873	G.J. Feldman, R.D. Cousins	
FUKUDA	98	PL B433 9	Y. Fukuda *et al.*	(Super-Kamiokande Collab.)
FUKUDA	98C	PRL 81 1562	Y. Fukuda *et al.*	(Super-Kamiokande Collab.)
FUKUDA	98E	PL B436 33	Y. Fukuda *et al.*	(Super-Kamiokande Collab.)
HAMPEL	98	PL B420 114	W. Hampel *et al.*	(GALLEX Collab.)
HATAKEYAMA	98	PRL 81 2016	S. Hatakeyama *et al.*	(Kamiokande Collab.)
OYAMA	98	PR D57 R6594	Y. Oyama	
ALLISON	97	PL B391 491	W.W.M. Allison *et al.*	(Soudan 2 Collab.)

CLARK	97	PRL 79 345	R. Clark *et al.*	(IMB Collab.)
ROMOSAN	97	PRL 78 2912	A. Romosan *et al.*	(CCFR Collab.)
ATHANASSO...	96	PR C54 2685	C. Athanassopoulos *et al.*	(LSND Collab.)
ATHANASSO...	96B	PRL 77 3082	C. Athanassopoulos *et al.*	(LSND Collab.)
BORISOV	96	PL B369 39	A.A. Borisov *et al.*	(SERP, JINR)
FUKUDA	96	PRL 77 1683	Y. Fukuda *et al.*	(Kamiokande Collab.)
FUKUDA	96B	PL B388 397	Y. Fukuda *et al.*	(Kamiokande Collab.)
GREENWOOD	96	PR D53 6054	Z.D. Greenwood *et al.*	(UCI, SVR, SCUC)
HAMPEL	96	PL B388 384	W. Hampel *et al.*	(GALLEX Collab.)
LOVERRE	96	PL B370 156	P.F. Loverre	
ACHKAR	95	NP B434 503	B. Achkar *et al.*	(SING, SACLD, CPPM, CDEF+)
AHLEN	95	PL B357 481	S.P. Ahlen *et al.*	(MACRO Collab.)
ATHANASSO...	95	PRL 75 2650	C. Athanassopoulos *et al.*	(LSND Collab.)
BAHCALL	95	PL B348 121	J.N. Bahcall, P.I. Krastev, E. Lisi	(IAS)
DAUM	95	ZPHY C66 417	K. Daum *et al.*	(FREJUS Collab.)
HILL	95	PRL 75 2654	J.E. Hill	(PENN)
MCFARLAND	95	PRL 75 3993	K.S. McFarland *et al.*	(CCFR Collab.)
VYRODOV	95	JETPL 61 163	V.N. Vyrodov *et al.*	(KIAE, LAPP, CDEF)
		Translated from ZETFP 61 161.		
DECLAIS	94	PL B338 383	Y. Declais *et al.*	
FUKUDA	94	PL B335 237	Y. Fukuda *et al.*	(Kamiokande Collab.)
SMIRNOV	94	PR D49 1389	A.Y. Smirnov, D.N. Spergel, J.N. Bahcall	(IAS+)
VIDYAKIN	94	JETPL 59 390	G.S. Vidyakin *et al.*	(KIAE)
		Translated from ZETFP 59 364.		
VILAIN	94C	ZPHY C64 539	P. Vilain *et al.*	(CHARM II Collab.)
FREEDMAN	93	PR D47 811	S.J. Freedman *et al.*	(LAMPF E645 Collab.)
GRUWE	93	PL B309 463	M. Gruwe *et al.*	(CHARM II Collab.)
BECKER-SZ...	92	PRL 69 1010	R.A. Becker-Szendy *et al.*	(IMB Collab.)
BECKER-SZ...	92B	PR D46 3720	R.A. Becker-Szendy *et al.*	(IMB Collab.)
BEIER	92	PL B283 446	E.W. Beier *et al.*	(KAM2 Collab.)
Also	94	PTRSL A346 63	E.W. Beier, E.D. Frank	(PENN)
BORODOV...	92	PRL 68 274	L. Borodovsky *et al.*	(COLU, JHU, ILL)
HIRATA	92	PL B280 146	K.S. Hirata *et al.*	(Kamiokande II Collab.)
KETOV	92	JETPL 55 564	S.N. Ketov *et al.*	(KIAE)
		Translated from ZETFP 55 544.		
CASPER	91	PRL 66 2561	D. Casper *et al.*	(IMB Collab.)
HIRATA	91	PRL 66 9	K.S. Hirata *et al.*	(Kamiokande II Collab.)
KUVSHINN...	91	JETPL 54 253	A.A. Kuvshinnikov *et al.*	(KIAE)
BATUSOV	90B	ZPHY C48 209	Y.A. Batusov *et al.*	(JINR, ITEP, SERP)
BERGER	90B	PL B245 305	C. Berger *et al.*	(FREJUS Collab.)
HIRATA	90	PRL 65 1297	K.S. Hirata *et al.*	(Kamiokande II Collab.)
VIDYAKIN	90	JETP 71 424	G.S. Vidyakin *et al.*	(KIAE)
		Translated from ZETF 98 764.		
AGLIETTA	89	EPL 8 611	M. Aglietta *et al.*	(FREJUS Collab.)
BAHCALL	89	Neutrino Astrophysics	J.N. Bahcall	(IAS)
Cambridge University Press				
BLUMENFELD	89	PRL 62 2237	B.J. Blumenfeld *et al.*	(COLU, ILL, JHU)
DAVIS	89	ARNPS 39 467	R. Davis, A.K. Mann, L. Wolfenstein	(BNL, PENN+)
OYAMA	89	PR D39 1481	Y. Oyama *et al.*	(Kamiokande II Collab.)
AFONIN	88	JETP 67 213	A.I. Afonin *et al.*	(KIAE)
		Translated from ZETF 94 1, issue 2.		
AMMOSOV	88	ZPHY C40 487	V.V. Ammosov *et al.*	(SKAT Collab.)
BERGSMA	88	ZPHY C40 171	F. Bergsma *et al.*	(CHARM Collab.)
BIONTA	88	PR D38 768	R.M. Bionta *et al.*	(IMB Collab.)
DURKIN	88	PRL 61 1811	L.S. Durkin *et al.*	(OSU, ANL, CIT+)
LOVERRE	88	PL B206 711	P.F. Loverre	(INFN)
AFONIN	87	JETPL 45 247	A.I. Afonin *et al.*	(KIAE)
		Translated from ZETFP 45 201.		
AHRENS	87	PR D36 702	L.A. Ahrens *et al.*	(BNL, BROW, UCI+)
BOFILL	87	PR D36 3309	J. Bofill *et al.*	(MIT, FNAL, MSU)
LOSECCO	87	PL B184 305	J.M. LoSecco *et al.*	(IMB Collab.)
TALEBZADEH	87	NP B291 503	M. Talebzadeh *et al.*	(BEBC WA66 Collab.)
VIDYAKIN	87	JETP 66 243	G.S. Vidyakin *et al.*	(KIAE)
		Translated from ZETF 93 424.		
ABRAMOWICZ	86	PRL 57 298	H. Abramowicz *et al.*	(CDHS Collab.)
AFONIN	86	JETPL 44 142	A.I. Afonin *et al.*	(KIAE)
		Translated from ZETFP 44 111.		

ALLABY	86	PL B177 446	J.V. Allaby *et al.*	(CHARM Collab.)
ANGELINI	86	PL B179 307	C. Angelini *et al.*	(PISA, ATHU, PADO+)
BERNARDI	86B	PL B181 173	G. Bernardi *et al.*	(CURIN, INFN, CDEF+)
BRUCKER	86	PR D34 2183	E.B. Brucker *et al.*	(RUTG, BNL, COLU)
USHIDA	86C	PRL 57 2897	N. Ushida *et al.*	(FNAL E531 Collab.)
ZACEK	86	PR D34 2621	G. Zacek *et al.*	(CIT-SIN-TUM Collab.)
AFONIN	85	JETPL 41 435	A.I. Afonin *et al.*	(KIAE)
		Translated from ZETFP 41 355.		
Also	85B	JETPL 42 285	A.I. Afonin *et al.*	(KIAE)
		Translated from ZETFP 42 230.		
AHRENS	85	PR D31 2732	L.A. Ahrens *et al.*	(BNL, BROW, KEK+)
BELIKOV	85	SJNP 41 589	S.V. Belikov *et al.*	(SERP)
		Translated from YAF 41 919.		
STOCKDALE	85	ZPHY C27 53	I.E. Stockdale *et al.*	(ROCH, CHIC, COLU+)
ZACEK	85	PL 164B 193	V. Zacek *et al.*	(MUNI, CIT, SIN)
BALLAGH	84	PR D30 2271	H.C. Ballagh *et al.*	(UCB, LBL, FNAL+)
BERGSMA	84	PL 142B 103	F. Bergsma *et al.*	(CHARM Collab.)
CAVAIGNAC	84	PL 148B 387	J.F. Cavaignac *et al.*	(ISNG, LAPP)
DYDAK	84	PL 134B 281	F. Dydak *et al.*	(CERN, DORT, HEIDH, SACL+)
GABATHULER	84	PL 138B 449	K. Gabathuler *et al.*	(CIT, SIN, MUNI)
STOCKDALE	84	PRL 52 1384	I.E. Stockdale *et al.*	(ROCH, CHIC, COLU+)
AFONIN	83	JETPL 38 436	A.I. Afonin *et al.*	(KIAE)
		Translated from ZETFP 38 361.		
BELENKII	83	JETPL 38 493	S.N. Belenky *et al.*	(KIAE)
		Translated from ZETFP 38 406.		
BELIKOV	83	JETPL 38 661	S.V. Belikov *et al.*	(SERP)
		Translated from ZETFP 38 547.		
TAYLOR	83	PR D28 2705	G.N. Taylor *et al.*	(HAWA, LBL, FNAL)
COOPER	82	PL 112B 97	A.M. Cooper *et al.*	(RL)
VUILLEUMIER	82	PL 114B 298	J.L. Vuilleumier *et al.*	(CIT, SIN, MUNI)
ARMENISE	81	PL 100B 182	N. Armenise *et al.*	(BARI, CERN, MILA+)
ASRATYAN	81	PL 105B 301	A.E. Asratyan *et al.*	(ITEP, FNAL, SERP+)
BAKER	81	PRL 47 1576	N.J. Baker *et al.*	(BNL, COLU)
Also	78	PRL 40 144	A.M. Cnops *et al.*	(BNL, COLU)
BOLIEV	81	SJNP 34 787	M.M. Boliev *et al.*	(INRM)
		Translated from YAF 34 1418.		
DEDEN	81	PL 98B 310	H. Deden *et al.*	(BEBC Collab.)
ERRIQUEZ	81	PL 102B 73	O. Erriquez *et al.*	(BARI, BIRM, BRUX+)
KWON	81	PR D24 1097	H. Kwon *et al.*	(CIT, ISNG, MUNI)
NEMETHY	81B	PR D23 262	P. Nemethy *et al.*	(YALE, LBL, LASL+)
SILVERMAN	81	PRL 46 467	D. Silverman, A. Soni	(UCI, UCLA)
USHIDA	81	PRL 47 1694	N. Ushida *et al.*	(AICH, FNAL, KOBE, SEOU+)
AVIGNONE	80	PR C22 594	F.T. Avignone, Z.D. Greenwood	(SCUC)
BOEHM	80	PL 97B 310	F. Boehm *et al.*	(ILLG, CIT, ISNG, MUNI)
FRITZE	80	PL 96B 427	P. Fritze (AACH3, BONN, CERN, LOIC, OXF+)	
REINES	80	PRL 45 1307	F. Reines, H.W. Sobel, E. Pasierb	(UCI)
Also	59	PR 113 273	F. Reines, C.L. Cowan	(LASL)
Also	66	PR 142 852	F.A. Nezrick, F. Reines	(CASE)
Also	76	PRL 37 315	F. Reines, H.S. Gurr, H.W. Sobel	(UCI)
DAVIS	79	PR C19 2259	R. Davis *et al.*	(CIT)
BLIETSCHAU	78	NP B133 205	J. Blietschau *et al.*	(Gargamelle Collab.)
CROUCH	78	PR D18 2239	M.F. Crouch *et al.*	(CASE, UCI, WITW)
BELLOTTI	76	LNC 17 553	E. Bellotti *et al.*	(MILA)